AD_____
(Leave blank)

Award Number: W81XWH-10-1-0442

TITLE: Specific Inhibitors of Histone Demethylases: Novel Chemical Agents for Breast Cancer Therapy

PRINCIPAL INVESTIGATOR: Liviu M. Mirica, PhD

CONTRACTING ORGANIZATION: Washington University
Saint Louis, MO 63130-4862

REPORT DATE: August 2012

TYPE OF REPORT: Final

PREPARED FOR: U.S. Army Medical Research and Materiel Command
Fort Detrick, Maryland 21702-5012

DISTRIBUTION STATEMENT: (Check one)

X Approved for public release; distribution unlimited

☐ Distribution limited to U.S. Government agencies only; report contains proprietary information

REPORT DOCUMENTATION PAGE

Form Approved
OMB No. 0704-0188

1. REPORT DATE *(DD-MM-YYYY)*	2. REPORT TYPE	3. DATES COVERED *(From - To)*
August 2012	Final	01 August 2010- 31 July 2012

4. TITLE AND SUBTITLE
Specific Inhibitors of Histone Demethylases: Novel Chemical Agents for Breast Cancer Therapy

5a. CONTRACT NUMBER
.

5b. GRANT NUMBER
W81XWH-10-1-0442

5c. PROGRAM ELEMENT NUMBER

6. AUTHOR(S)
Liviu M. Mirica, PhD
Barbara Cascella (née Gordon)

5d. PROJECT NUMBER

5e. TASK NUMBER

5f. WORK UNIT NUMBER

7. PERFORMING ORGANIZATION NAME(S) AND ADDRESS(ES)
Washington University,

Saint Louis, MO 63130-4862

8. PERFORMING ORGANIZATION REPORT NUMBER

9. SPONSORING / MONITORING AGENCY NAME(S) AND ADDRESS(ES)
U.S. Army Medical Research and Materiel Command
Fort Detrick, Maryland 21702-5012

10. SPONSOR/MONITOR'S ACRONYM(S)

11. SPONSOR/MONITOR'S REPORT NUMBER(S)

12. DISTRIBUTION / AVAILABILITY STATEMENT
Approved for public release; distribution unlimited

13. SUPPLEMENTARY NOTES

14. ABSTRACT
Histone demethylases are a newly discovered class of non-heme iron enzymes that play an important role in regulating transcription and epigenetic inheritance. We have successfully expressed and purified highly active histone demethylases (HDMs), including the cancer-relevant JMJD2C (GASC1). A detailed enzyme kinetic and inhibition analysis of these HDMs was achieved through a range of fluorescence assays, mass spectrometry, and oxygen consumption measurements. An interesting case of cosubstrate inhibition is observed for these HDMs, with direct relevance to the potential role of alpha-ketoglutarate and HDMs in cancer cells. We have also employed an enzyme-templated approach for specific inhibitor design that takes advantage of the enzyme's substrate specificity. Finally, while the initially tested compounds do not seem to inhibit JMJD2C in MCF7 breast cancer cells, we believe that second generation compounds will be active HDM inhibitors in vivo. The developed specific inhibitors could lead to novel breast cancer therapeutics and can also be used as tools for studying the role of histone demethylases in breast cancer cell proliferation.

15. SUBJECT TERMS
Epigenetics, histone demethylases, inhibitor design, GASC1 oncogene

16. SECURITY CLASSIFICATION OF:			17. LIMITATION OF ABSTRACT	18. NUMBER OF PAGES	19a. NAME OF RESPONSIBLE PERSON
a. REPORT	b. ABSTRACT	c. THIS PAGE			USAMRMC
U	U	U	UU	44	19b. TELEPHONE NUMBER *(include area code)*

Table of Contents

Introduction

Covalent modification of chromatin by histone methylation has wide-ranging effects on nuclear functions, such as transcriptional regulation, genome integrity, and epigenetic inheritance.[1] Until recently, histone methylation was considered a static modification, but the identification of histone demethylase (HDM) enzymes has revealed that this mark is dynamically controlled.[2] Most of the identified histone demethylases are α-ketoglutarate (α-KG) dependent, O_2-activating non-heme iron enzymes (Figure 1) that catalyze the lysine demethylation through a hydroxylation reaction (Scheme 1).[3]

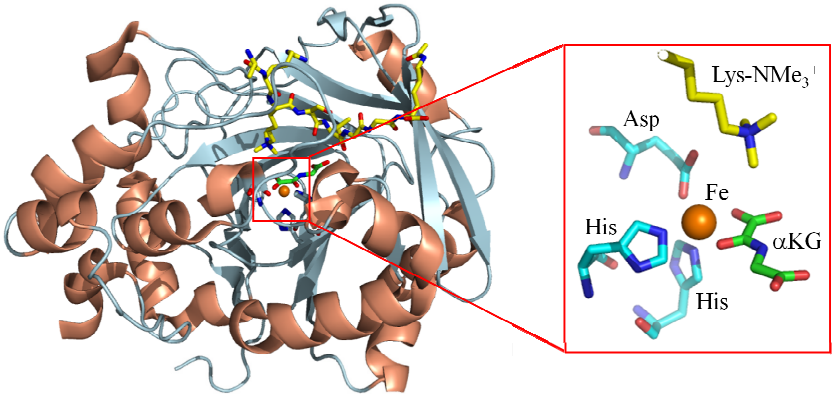

Figure 1. Crystal structure of JMJD2A, a JmjC-domain histone demethylase (HDM).[4]

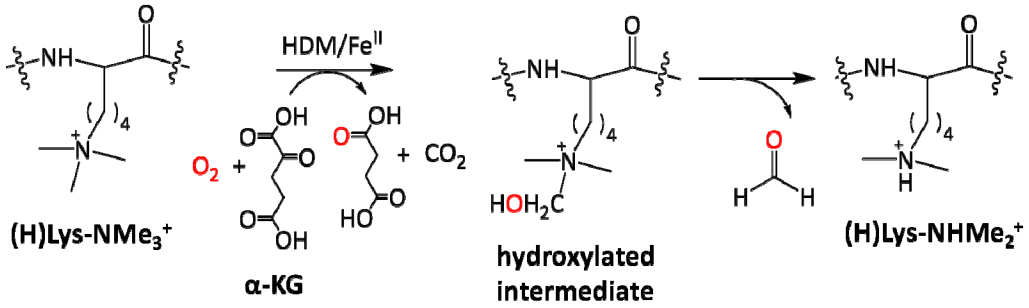

Scheme 1. Histone demethylation reaction catalyzed by HDMs.

It has recently been shown that the histone demethylase GASC1 (or JMJD2C) is overexpressed in several cancer cells and may be linked to the stem cell phenotypes in breast cancer.[5] In addition, the histone demethylase PLU-1 plays an important role in the proliferation of breast cancer cells through transcriptional repression of tumor suppressor genes.[6] Thus, the development of specific inhibitors for HDMs could provide new avenues for breast cancer therapeutic development. Our approach will employ the design of specific inhibitors of histone demethylases using a novel enzyme-templated Huisgen 1,3-dipolar cycloaddition reaction between the azide adduct of the targeted enzyme and an alkyne substrate analog (Scheme 2). The cycloaddition reaction should proceed at a faster rate than in solution, due to the sequestering of the two components in the enzyme active site. Thus, the enzyme itself, serving as the reaction vessel, is synthesizing its highest-affinity inhibitor. The synthesized compounds will mimic two substrates (O_2 and the methylated amine substrate) and most likely be specific for the targeted enzyme.

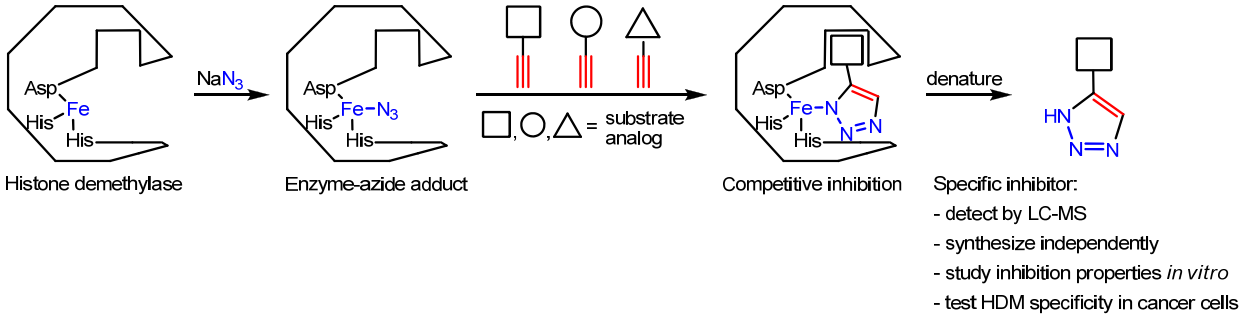

Scheme 2. Enzyme-templated approach for development of specific competitive inhibitors.

Body

Despite the important role of the recently discovered HDMs in epigenetics and cancer biology, there are limited data available on the enzymology of HDMs. In this regard, we have successfully expressed and purified three HDMs, including the cancer-relevant JMJD2C, and obtained a detailed enzyme kinetic analysis by employing three different assays. Our initial kinetic studies focused on JMJD2A, the first HDM with a resolved crystal structure and one that has been used extensively in biochemical studies.[4] The pseudogene-encoded JMJD2E, which shares greater than 80% sequence similarity to JMJD2A, has been often employed in enzyme activity studies as it has the highest activity when compared to the other members of the JMJD2 subfamily.[7,8a,b] Finally, JMJD2C is of great interest due to its implications in brain, breast, prostate, and esophageal cancers,[5,9] although the kinetics of JMJD2C has not been fully investigated to date.[7,8c,d,e]

Task 2a: *HDM expression and purification*. Truncated constructs of JMJD2A, [4b] JMJD2E, [7,8a] and JMJD2C[7,8d] containing the JmjN- and JmjC-domains were transformed into the *E. coli* Rosetta II strain and expressed and purified using published procedures.[4,7,8] Purification was achieved via Ni-NTA superflow and anion-exchange column chromatography to yield enzymes with >90% purity and expression yields of ~5 mg/L for JMJD2A and JMJD2C and ~20 mg/L for JMJD2E. The enzymatic activity of the three HDMs was monitored by three complimentary assays: a coupled formaldehyde dehydrogenase (FDH) NADH fluorescence assay, a discontinuous MALDI-TOF mass spectrometry (MS) assay, and a continuous O_2 consumption assay.

Tasks 3a-b: *Fluorescence coupled assay*. Using a modified coupled assay,[4c,10] the HDM activity was monitored via the production of fluorescent NADH formed during formaldehyde oxidation by a formaldehyde dehydrogenase coupled reaction (Figure 2). In all enzymatic assays, an octapeptide (ARK(me_3)STGGK) corresponding to the histone sequence around the methylated lysine was employed as the substrate analog.

Oxygen consumption assay. No direct continuous assay to study the enzymatic activity of HDMs has been developed to date. In this regard, we have employed a continuous O_2 consumption assay that measures in real-time the HDM enzymatic activity through the use of a Clark oxygen electrode.[11] This allowed us to obtain a detailed characterization of the enzymatic kinetic properties of the three HMDs investigated (see below).

MALDI-TOF assay. Demethylation of the peptide substrate was also confirmed by mass spectrometry (MALDI-TOF). The amount of the mono- and di-methylated peptide was

determined at the end of the reaction, converted to percent conversion of peptide substrate and used to correlate the extent of demethylation with the other enzymatic assays.

Using the above enzyme activity assays, we have determined the kinetic parameters for the three HDMs with respect to all three substrates: the ARK(me_3)STGGK peptide substrate, O_2, and αKG. For JMJD2A and JMJD2C, The FDH coupled assay yielded K_m values for the peptide substrate (104 ± 16 μM for JMJD2A, 76 ± 11 μM for JMJD2C) that are similar to those found in the literature,[4a,7,8e,12] while for JMJD2E a slightly larger K_m value was obtained (224 ± 15 μM, Table 1).[13] Interestingly, the use of the O_2 consumption assay reveals significantly reduced peptide K_m values for JMJD2A (31 ± 3 μM), JMJD2E (38 ± 3 μM), and JMJD2C (32 ± 3 μM), as well as turnover numbers that are similar or higher than those from other studies.[4a,7,8e,12] The O_2 consumption assays can be performed under saturating conditions for all substrates and thus it provides a unique opportunity of obtain true k_{cat} values for the three HMDs (Table 1). Most importantly, the observed activity of JMJD2C is higher than reported previously[7,8e] and comparable to those of JMJD2A and JMJD2E, the HDMs commonly used in enzyme activity studies.[7,8] Thus, JMJD2C can now be used in inhibition studies employing the O_2 consumption assay, especially given its direct implication in cancer biology.[5] Overall, the O_2 consumption assay seems to allow for a superior characterization of HDMs vs. the FDH coupled assay, since the obtained K_m values for the peptide substrate are more in line with the expected affinities for the natural substrate *in vivo*, while higher turnover numbers were also found for all three HDMs investigated.[13]

Table 1. Kinetic parameters for the three HDMs JMJD2A, JMJD2E, and JMJD2C.

Substrate Kinetic parameters		***H3K9me₃*** K_m^{app}(μM), k_{cat}^{app} (min^{-1})[a]	***O₂*** K_m^{app} (μM), k_{cat}^{app} (min^{-1})	***αKG*** K_m^{app} (μM), K_i^{app} *(mM)*[d]
HDM	Assay			
JMJD2A	O_2 consumed	31 ± 3, 2.5 ± 0.1[a]	57 ± 10, 2.5 ± 0.1	10 ± 1, *10 ± 2*[d]
	coupled FDH	104 ± 16, 1.4 ± 0.1[b]	N.M.[c]	21 ± 4, *13 ± 3*[d]
JMJD2E	O_2 consumed	38 ± 3, 3.3 ± 0.1[b]	197 ± 16, 4.0 ± 0.1	21 ± 2, *12 ± 1*[d]
	coupled FDH	224 ± 15, 2.1 ± 0.1[b]	N.M.[c]	37 ± 7, *11 ± 3*[d]
JMJD2C	O_2 consumed	32 ± 3, 2.1 ± 0.1[b]	158 ± 13, 2.6 ± 0.1	12 ± 2, *4.3 ± 0.6*[d]
	coupled FDH	76 ± 11, 0.70 ± 0.03[b]	N.M.[c]	22 ± 5, *3.4 ± 0.6*[d]

[a] k_{cat}^{app} values were determined at 258 μM O_2. [c] Not measured. [d] αKG K_i^{app} values reported at 258 μM O_2.

Using the O_2 consumption assay, we have measured for the first time the $K_m(O_2)$ values for HDMs and found that these enzymes have relatively low apparent affinities for O_2, with K_m values near or above normal cellular O_2 concentration (57 ± 10 μM for JMJD2A; 197 ± 16 μM for JMJD2E; 158 ± 13 μM for JMJD2C, Figure 2).[14] Such O_2 affinities suggest the enzymatic activity can be altered by small changes in O_2 concentration, and thus the HDMs can act as

oxygen sensors *in vivo*, as observed previously for other αKG-dependent non-heme iron oxygenases involved in the hypoxic response.[14]

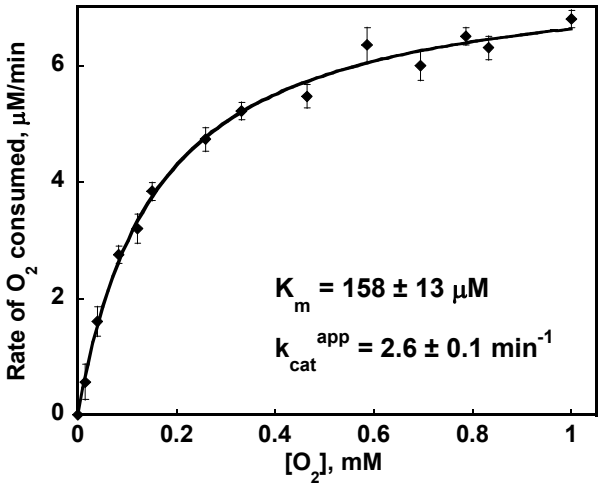

Figure 2. Michaelis-Menten plot for JMJD2C obtained using a Clark oxygen electrode and varying O_2 concentrations. Reaction conditions: 50 mM HEPES pH 7.5, 100 μM ARK(me_3)STGGK, 300 μM αKG, 500 μM ascorbate, 3 μM $Fe^{II}(NH_4)_2SO_4 \bullet 6H_2O$, 3 μM JMJD2C, 15 μM - 1 mM O_2, 25 °C.

While investigating the affinities of JMJD2A and JMJD2E for αKG, a mild substrate inhibition effect was found when αKG was present in high concentrations (>1 mM).[13] The apparent K_i values were obtained using the FDH coupled assay (JMJD2A, K_i^{app} = 13 ± 3 mM; JMJD2E, K_i^{app} = 11 ± 3 mM) and the O_2 consumption assay (JMJD2A, K_i^{app} = 10 ± 2 mM; JMJD2E, K_i^{app} = 12 ± 1 mM, Table 1). Interestingly, the αKG inhibitory effect is significantly stronger in the case of JMJD2C (FDH coupled assay: K_i^{app} = 3.4 ± 0.6 mM, Figure 3; O_2 electrode assay: K_i^{app} = 4.3 ± 0.6 mM). The inhibition of JMJD2C by αKG was measured at constant αKG concentrations (300 μM, 2 mM, 4 mM, 5 mM) and variable O_2 concentrations using the O_2 consumption assay. It was found that the K_m value for O_2 increased with increasing αKG concentration, while the V_{max} value stayed relatively constant.[13] In addition, a double reciprocal plot of the inverse of rate of reaction vs. the inverse of O_2 concentration reveals that the linear plots corresponding to the different αKG concentrations intersect on the y-axis, suggesting that αKG is a competitive inhibitor with respect to O_2 (Figure 4).

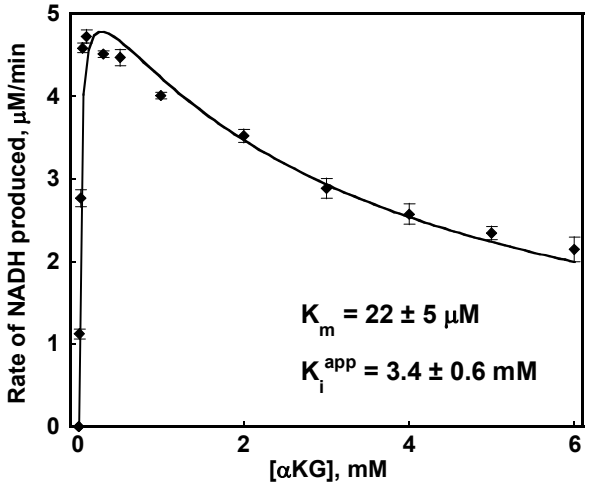

Figure 3. Inhibition of JMJD2C by αKG, measured by the FDH coupled assay. Reaction conditions: 50 mM HEPES pH 7.5, 250 μM ARK(me_3)STGGK, 500 μM ascorbate, 1 mM NAD^+, 0.04 units FDH, 50 mM NaCl, 50 μM $Fe^{II}(NH_4)_2SO_4 \cdot 6H_2O$, 8 μM JMJD2C, 258 μM O_2, 25 °C.

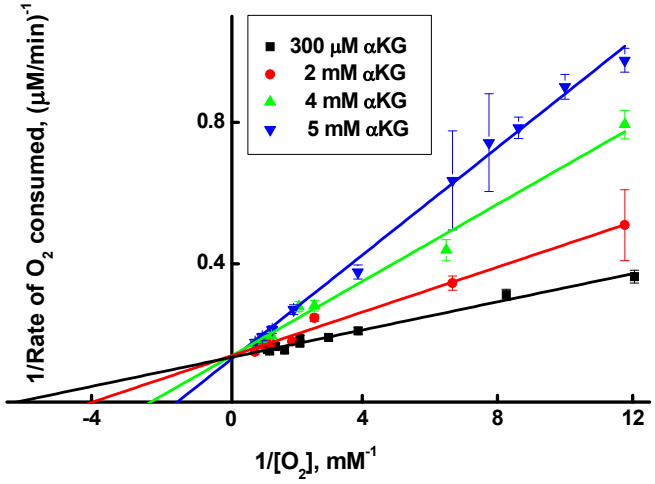

Figure 4. Double reciprocal plot of 1/rate of O_2 consumed vs. 1/[O_2] obtained using the O_2 consumption assay, suggesting αKG competitive inhibition of JMJD2C with respect to O_2.

Novel finding: The observed αKG substrate inhibition of JMJD2C could have important implications in cancer biology, as JMJD2C is encoded by the putative oncogene GASC1 that is implicated in various types of cancer.[9] In normal healthy cells, the expression and activity of JMJD2C is believed to be highly regulated.[5,9] Given the observed *in vitro* inhibition by αKG, the activity of JMJD2C could be regulated in healthy tissue through a high cellular concentration of αKG, which does not allow for an optimal demethylase activity of JMJD2C. Interestingly, there is a large difference in the level of αKG in healthy brain cells and glioblastomas. Whereas in healthy brain tissue the αKG concentration ranges from 1 to 3 mM,[15] it has been reported that the αKG concentration in gliomas and glioblastoma multiformes is 100-300 μM.[16] Indeed, we find that JMJD2C displays its highest activity *in vitro* at an αKG concentration of ~300 μM,[13] suggesting that a decreased concentration of αKG could lead to an increased HDM activity in

cancer vs. normal cells.[17] Thus, we plan to further study the implication of the observed αKG substrate inhibition for HMDs and the effect of αKG concentration variation in cancer cells.

Task 1b and 2b: *Inhibitor synthesis and evaluation.* We have began our inhibitor development studies by synthesizing a large number of substrate analogs bearing either di- and tri-methylammonium groups or α-keto-acid fragments (Chart 1) to be tested for their inhibition properties. A representative synthetic scheme is shown in Scheme 3 for compound (2b), 2-oxo-2-propynylamino-acetic acid, PgAmideAcid.

Compound	Structure
(2a) ethyl 2-oxo-2-(prop-2-ynylamino) acetate	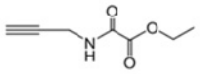
(2b) 2-oxo-2-(propynylamino) acetic acid	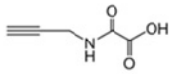
(3) dimethyl ammonium alkyne ester	
(4) trimethyl ammonium alkyne ester	
(5) trimethyl ammonium propyne	
(6) trimethyl ammonium butyne	
(7) trimethyl ammonium hexyne	
(8) methyl 4-((dimethylamino)methyl)-1H-1,2,3-triazole-5-carboxylate	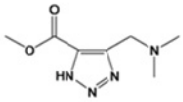
(9) 1-(5-(methoxycarbonyl)-1H-1,2,3-triazol-4-yl)-N,N,N-trimethylmethanaminium	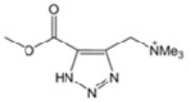
(10) *N,N,N*-trimethyl-1-(1*H*-1,2,3-triazol-4-yl)methanaminium	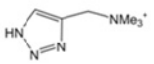
(11) *N,N,N*-trimethyl-2-(1*H*-1,2,3-triazol-4-yl)ethanaminium	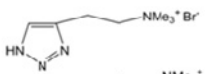
(12) *N,N,N*-trimethyl-4-(1*H*-1,2,3-triazol-4yl)butan-1-aminium	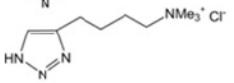

Chart 1. List of synthesized substrate analogs for HDM inhibition studies.

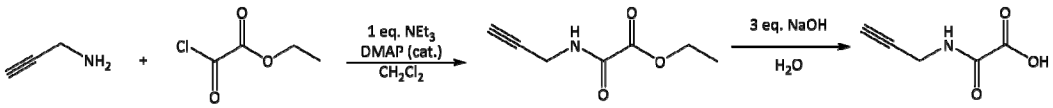

Scheme 3. Synthesis of an *N*-oxalylglycine (NOG) alkyne analog, PgAmideAcid.

Task 3b: The synthesized substrate analogs were then tested for their inhibition properties against the three HMDs. The inhibitory properties of our compounds were determined using Dixon plots (Figure 5) to obtain the apparent inhibition constants, K_i's. We use K_i rather than IC_{50} values as K_i is an absolute value and IC_{50} is substrate- and enzyme-concentration dependent. While the analogs containing trimethylammonium groups show a mild inhibition of JMJD2A and JMJD2E (Table 2), the αKG analogs such as *N*-oxalylglycine (NOG) are good yet unspecific inhibitors of HDMs. By contrast, the designed alkyne NOG analog (PgAmideAcid) shows good affinity for JMJD2E and this compound was used in the enzyme-templated cycloaddition reaction (see below).

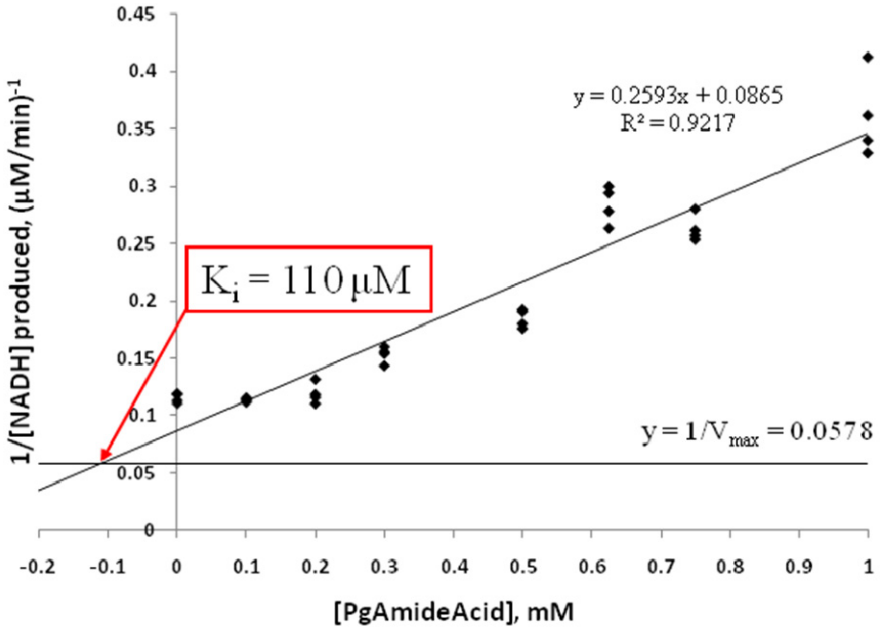

Figure 5. Dixon plot of JMD2E inhibition by PgAmideAcid.

Table 2. Summary of inhibition data for the initially developed compounds.

Inhibitor	Structure	Ki (apparent)
N-oxalylglycine	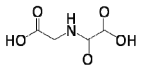	208µM
Propargyl AmideAcid	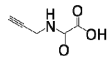	110µM
Pyridine AmideAcid	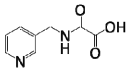	215µM
2,4-Pyridine dicarboxylic acid	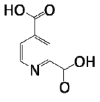	6µM
NMe_3^+ OMe alkyne	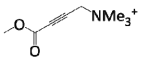	571µM
NMe_3^+ Triazole	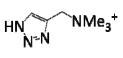	1.18mM

Task 3d: We are currently developing second generation compounds that are αKG substrate analogs and thus are expected to increase the affinity toward HDMs (Chart 2). In addition, these compounds contain alkyne, triazole, and/or trimethylammonium molecular fragments that should confer specificity for various HDMs, depending on how these molecules are expected to fit in the active site and act as inhibitors with respect to the peptide substrate, O_2, as well as αKG. Moreover, the alkyne-containing compounds will be employed in enzyme-templated cycloaddition studies for generation of triazole-containing compounds with an increased affinity for the targeted HDM (see below). inhibition propertie motif, in order to take advantage of the observed substrate inhibition behavior, evaluate their inhibition properties in vitro, followed by cellular studies.

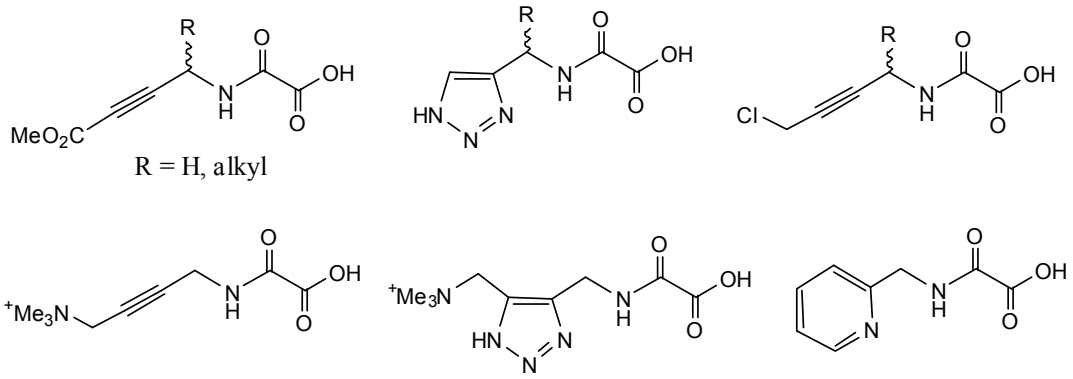

Chart 2. List of second generation αKG substrate analogs for HDM inhibition studies.

Task 2c-e: *Enzyme-templated cycloaddition reaction.* The alkyne NOG analog PgAmideAcid that shows affinity for the HMDs was employed in the enzyme-templated cycloaddition studies. Preliminary results suggest that in presence of JMJD2E, PgAmideAcid reacts with azide to form the corresponding triazole product, as observed by ESI-MS (Figure 6). This promising result takes advantage of the enzyme's ability to bind both substrate analogs and promote the cycloaddition reaction. We are currently synthesizing the identified triazole product in larger quantities using organic synthesis and will test its inhibitory properties against HDMs.

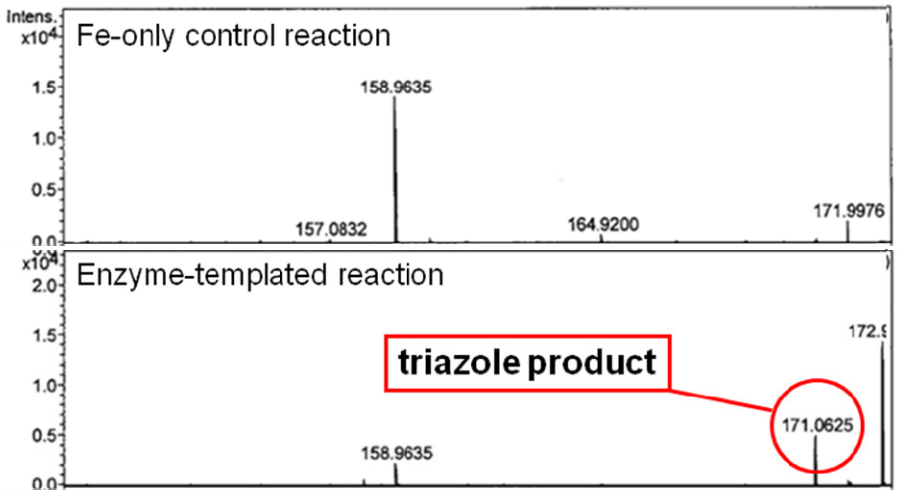

Figure 6. The observed enzyme-templated cycloaddition reaction and ESI-MS evidence for product formation.

Task 2c: We are employing the enzyme-templated cycloaddition reaction as a means of detection of lead compounds that are expected to be good inhibitors for HDMs. Based on the results obtained from the small molecule mimics studies (**Task 1d**), we are currently employing Co- and Ni-reconstituted HDMs for the enzyme-templated synthesis of triazole compounds in an attempt to detect inhibitors of various efficacy and specificity. Preliminary results suggest that such HDMs should facilitate the targeted enzyme-templated cycloaddition reactions.

Task 1a-d: Concurently with the enzyme kinetic and inhibition studies and the enzyme-templated cycloaddition reaction studies, we have also investigated the 1,3-dipolar cycloaddition reaction between metal-azide complexes and alkyne reagents, i.e. an inorganic variant of the extensively used "click reaction". In this context, we have synthesized small molecule models of the metal active sites of HDMs and investigated the cycloaddition reaction between the azide adducts of these complexes and various alkynes to determine the scope of the reaction with respect to the alkyne and metal compound properties. The reaction between the azide complexes of bioinorganic metals (e.g. Fe, Co, Ni) that are models of metalloenzymes and alkyne reagents is envisioned as a potential new method of developing triazole-based specific inhibitors for HMDs in particular, and for other O_2-activating metalloenzymes in general.

The synthesis and characterization of six Fe, Co, and Ni mono-azide complexes has been accomplished using salen- and cyclam-type ligands (Scheme 3).[18] Then the scope of the inorganic azide-alkyne "click reaction" was investigated using the electron deficient alkyne dimethyl acetylenedicarboxylate. Of the six metal complexes investigated, only the Co and Ni azide complex of the tetra-methylcyclam ligand showed a successful cycloaddition reaction and formation of the corresponding metal-triazolate products that were crystallographically characterized (Scheme 4).[18] Moreover, use of a large number of synthesized alkynes that did not yield any cycloaddition reaction product (data not shown), suggesting that an electron deficient is required for the cycloaddition reaction to occur for an inorganic complex. However, the enzyme-templated cycloaddition reaction is expected to occur for a large number of alkyne substrates (see above) due to the enzyme's ability to sequester the two substrates and promote the triazole formation.

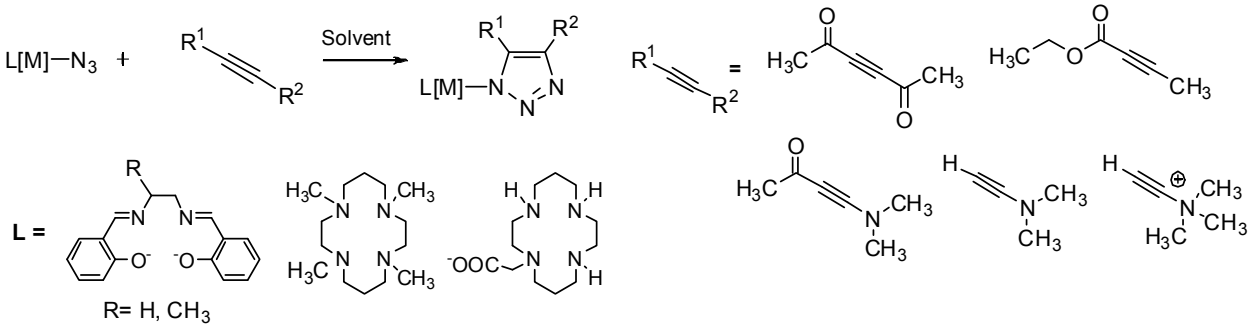

Scheme 3. The scope of the studied cycloaddition reaction between metal-azide complexes and various alkynes for the synthesis of metal-triazolate complexes.

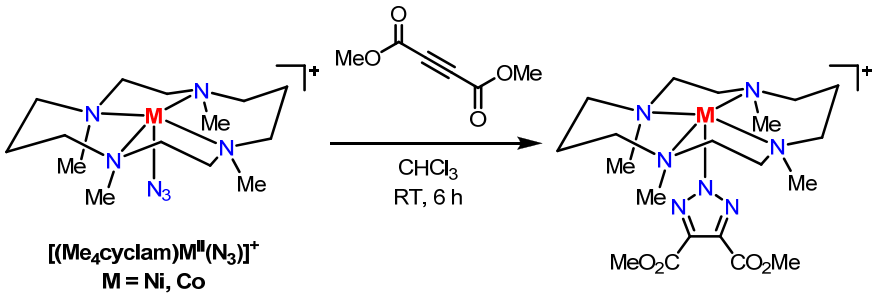

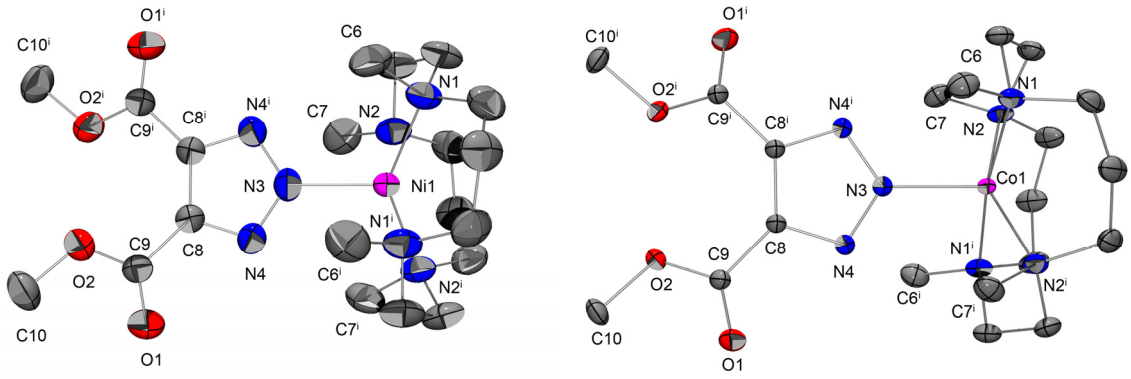

Scheme 4. Successful cycloaddition reaction between metal-azide complexes and dimethyl acetylenedicarboxylate and crystal structures of the Co- and Ni-triazolate complexes.

Overall, these results reveal that the success of the cycloaddition reaction between a metal-azide complex and an alkyne substrate is dependent both on the ligand and metal oxidation state of the metal complex, and the electron deficient nature of the alkyne employed. We plan to use the azide complexes that show efficient triazole formation as a method of synthesizing larger quantities of the triazoles that show promising inhibitory properties (**Task 3d**).

Task 4: Unfortunately, the first generation compounds that we developed (shown in Table 3) do not exhibit low K_i values toward HDMs, and thus are expected to not be potent inhibitors *in vivo*. Indeed, even the highest affinity inhibitor, 2,4-pyridine dicarboxylic acid, was reported

previously to not affect the growth of cancer cells [8], and our initial studies confirm these results. However, while the first generation compounds do not seem to inhibit JMJD2C in cancer cells, we expect that the second generation compounds, which were designed as inhibitors with respect to two or three substrates will be potent HDM inhibitors *in vivo*. Thus, we will use HCC1954 breast cancer cells (that show overexpression of GASC1 histone demethylase) and test the cell growth in presence of our newly developed compounds. In addition, we will probe the role of GASC1 inhibition in cancer cells by comparing the observed effects when treating with histone demethylase inhibitors the HCC1954 cells vs. MCF10A cells (that do not overexpress GASC1).

Future Directions

We plan to express and purify a series of other HDMs that have various histone tail specificity. Then we will use our developed compounds and evaluate their inhibition properties versus these HDMs, in order to determine the chemical factors that confer inhibition specificity toward various HDMs. In addition, we will employ the enzyme-templated cycloaddition strategy to develop novel compounds that have increased inhibitory properties and ideally are specific for a particular HDM. Finally, the generated compounds will be evaluated for their ability to inhibit HDMs in living cells, in order to identify the compounds that can control the activity of HDMs in cancer cells. Such compounds could be used to study the role of HDMs in breast cancer and serve as lead compounds for the development of novel anti-cancer therapies.

Key research accomplishments

- Expressed and purified three highly active histone demethylases (HDMs).
- Developed a continuous oxygen consumption assay for monitoring the activity of HDMs in real time.
- Obtained a detailed kinetic characterization of the targeted HDMs, including the first enzymatic activity analysis of the cancer-relevant JMJD2C.
- Discovered a unique case of cosubstrate inhibition of JMD2C, which is likely relevant to the role of HDMs in cancer cells.
- Developed a series of substrate analogs that exhibit HDM inhibition properties and set the stage for the design of specific inhibitors.
- Provide the proof of concept for the targeted enzyme-templated cycloaddition reaction for the development of specific HDM inhibitors.

Reportable Outcomes

Meeting Abstract

Barbara Cascella and Liviu M. Mirica * *"*Development of Specific Inhibitors for JmjC-Domain Histone Demethylases*"*, poster presentation, *46th Midwest Regional Meeting of the American Chemical Society*, St. Louis, October 2011

Barbara S. Gordon and Liviu M. Mirica,* "Development of Specific Inhibitors for Histone Demethylases", poster presentation, *Era of HOPE conference, DOD CMDRP program*, August 2-5, Orlando Florida.

Published manuscripts (attached as appendices)

Cascella, B.; Mirica, L. M.* "Kinetic Analysis of Iron-Dependent Histone Demethylases: α-Ketoglutarate Substrate Inhibition and Potential Relevance to the Regulation of Histone Demethylation in Cancer Cells", *Biochemistry*, **2012**, *51*, 8699-8701, DOI: 10.1021/bi3012466

Evangelio, E.; Rath, N. P.; Mirica, L. M.* "Cycloaddition Reactivity Studies of First Row Transition Metal-Azide Complexes and Alkynes: An Inorganic Click Reaction for Metalloenzyme Inhibitor Synthesis", *Dalton Trans.*, **2012**, *41*, 8010-8021, DOI: 10.1039/C2DT30145H

Conclusion

Histone demethylases are a newly discovered class of non-heme iron enzymes that play an important role in regulating transcription and epigenetic inheritance. We have successfully expressed and purified highly active histone demethylases (HDMs), including the cancer-relevant JMJD2C (GASC1). A detailed enzyme kinetic and inhibition analysis of these HDMs was achieved through a range of fluorescence assays, mass spectrometry and oxygen consumption measurements. An interesting case of cosubstrate inhibition is observed for these HDMs. We have also provided evidence for a novel enzyme-templated synthetic approach that takes advantage of the enzyme's substrate specificity to develop specific inhibitors for these enzymes. The developed specific inhibitors could lead to novel breast cancer therapeutics and can also be used as tools for studying the role of histone demethylases in breast cancer cell proliferation.

References

(1) Klose, R. J.; Kallin, E. M.; Zhang, Y. *Nat. Rev. Gen.* **2006**, *7*, 715-727; b) Bhaumik, S. R.; Smith, E.; Shilatifard, A. *Nat. Struct. & Mol. Biol.* **2007**, *14*, 1008-1016; b) Mosammaparast, N.; Shi, Y. *Annu. Rev. Biochem* **2010**, *79*, 155-179.

(2) Klose, R. J.; Yamane, K.; Bae, Y. J.; Zhang, D. Z.; Erdjument-Bromage, H.; Tempst, P.; Wong, J. M.; Zhang, Y. *Nature* **2006**, *442*, 312-316; b) Tsukada, Y.; Fang, J.; Erdjument-Bromage, H.; Warren, M. E.; Borchers, C. H.; Tempst, P.; Zhang, Y. *Nature* **2006**, *439*, 811-816; b) Zhang, Y.; Klose, R. J. *Nat. Rev. Mol. Cell Biol.* **2007**, *8*, 307-318.

(3) Costas, M.; Mehn, M. P.; Jensen, M. P.; Que, L., Jr. *Chem. Rev.* **2004**, *104*, 939-986; b) Krebs, C.; Fujimori, D. G.; Walsh, C. T.; Bollinger, J. M., Jr. *Acc. Chem. Res.* **2007**, *40*, 484-492; b) Loenarz, C.; Schofield, C. J. *Trends Biochem. Sci* **2011**, *36*, 7-18.

(4) Chen, Z.; Zang, J.; Whetstine, J.; Hong, X.; Davrazou, F.; Kutateladze, T. G.; Simpson, M.; Mao, Q.; Pan, C. H.; Dai, S.; Hagman, J.; Hansen, K.; Shi, Y.; Zhang, G. *Cell* **2006**, *125*, 691-702; b) Ng, S. S. et al. *Nature* **2007**, *448*, 87-U88; b) Couture, J. F.; Collazo, E.; Ortiz-Tello, P. A.; Brunzelle, J. S.; Trievel, R. C. *Nat. Struct. & Mol. Biol.* **2007**, *14*, 689-695.

(5) Cloos, P. A. C.; Christensen, J.; Agger, K.; Maiolica, A.; Rappsilber, J.; Antal, T.; Hansen, K. H.; Helin, K. *Nature* **2006**, *442*, 307-311.
(6) Lu, P. J.; Sundquist, K.; Baeckstrom, D.; Poulsom, R.; Hanby, A.; Meier-Ewert, S.; Jones, T.; Mitchell, M.; Pitha-Rowe, P.; Freemont, P.; Taylor-Papadimitriou, J. *J. Biol. Chem.* **1999**, *274*, 15633-15645; b) Yamane, K.; Tateishi, K.; Klose, R. J.; Fang, J.; Fabrizio, L. A.; Erdjument-Bromage, H.; Taylor-Papadimitriou, J.; Tempst, P.; Zhang, Y. *Mol. Cell* **2007**, *25*, 801-812.
(7) Rose, N. R.; Ng, S. S.; Mecinovic, J.; Lienard, B. M. R.; Bello, S. H.; Sun, Z.; McDonough, M. A.; Oppermann, U.; Schofield, C. J. *J. Med. Chem.* **2008**, *51*, 7053-7056; b) Rose, N. R.; Woon, E. C. Y.; Kingham, G. L.; King, O. N. F.; Mecinovic, J.; Clifton, I. J.; Ng, S. S.; Talib-Hardy, J.; Oppermann, U.; McDonough, M. A.; Schofield, C. J. *J. Med. Chem.* **2010**, *53*, 1810-1818; b) Hamada, S.; Kim, T. D.; Suzuki, T.; Itoh, Y.; Tsumoto, H.; Nakagawa, H.; Janknecht, R.; Miyata, N. *Bioorg. Med. Chem. Lett.* **2009**, *19*, 2852-2855; b) Chang, K.-H.; King, O. N. F.; Tumber, A.; Woon, E. C. Y.; Heightman, T. D.; McDonough, M. A.; Schofield, C. J.; Rose, N. R. *ChemMedChem* **2011**, *6*, 759-764; b) Lohse, B.; Nielsen, A. L.; Kristensen, J. B. L.; Helgstrand, C.; Cloos, P. A. C.; Olsen, L.; Gajhede, M.; Clausen, R. P.; Kristensen, J. L. *Angew. Chem. Int. Ed.* **2011**, *123*, 9266-9269; b) Luo, X.; Liu, Y.; Kubicek, S.; Myllyharju, J.; Tumber, A.; Ng, S.; Che, K. H.; Podoll, J.; Heightman, T. D.; Oppermann, U.; Schreiber, S. L.; Wang, X. *J. Am. Chem. Soc.* **2011**, *133*, 9451-9456; b) Woon, E. C. Y. et al. *Angew. Chem. Int. Ed.* **2012**, *51*, 1631-1634; b) Rose, N. R.; McDonough, M. A.; King, O. N. F.; Kawamura, A.; Schofield, C. J. *Chem. Soc. Rev.* **2011**, *40*, 4364-4397.
(8) Hamada, S. et al. *J. Med. Chem.* **2010**, *53*, 5629-5638.
(9) Liu, G.; Bollig-Fischer, A.; Kreike, B.; van de Vijver, M. J.; Abrams, J.; Ethier, S. P.; Yang, Z. Q. *Oncogene* **2009**, *28*, 4491-4500.
(10) Shi, Y.; Lan, F.; Matson, C.; Mulligan, P.; Whetstine, J. R.; Cole, P. A.; Casero, R. A.; Shi, Y. *Cell* **2004**, *119*, 941-953; b) Roy, T. W.; Bhagwat, A. S. *Nucleic Acids Res.* **2007**, *35*.
(11) Mirica, L. M.; Klinman, J. P. *Proc. Natl. Acad. Sci. U. S. A.* **2008**, *105*, 1814-1819.
(12) Krishnan, S.; Collazo, E.; Ortiz-Tello, P. A.; Trievel, R. C. *Anal. Biochem.* **2012**, *420*, 48-53; b) Kristensen, L. H.; Nielsen, A. L.; Helgstrand, C.; Lees, M.; Cloos, P.; Kastrup, J. S.; Helin, K.; Olsen, L.; Gajhede, M. *FEBS J.* **2012**, *279*, 1905-1914.
(13) Cascella, B.; Mirica, L. M. *Biochemistry* **2012**, *51*, 8699−8701.
(14) Hirsila, M.; Koivunen, P.; Gunzler, V.; Kivirikko, K. I.; Myllyharju, J. *J. Biol. Chem.* **2003**, *278*, 30772-30780.
(15) Thirstrup, K.; Christensen, S.; Moller, H. A.; Ritzen, A.; Bergstrom, A. L.; Sager, T. N.; Jensen, H. S. *Pharmacol. Res.* **2011**, *64*, 268-273.
(16) Dang, L. et al. *Nature* **2009**, *462*, 739-744; b) Gross, S.; Cairns, R. A.; Minden, M. D.; Driggers, E. M.; Bittinger, M. A.; Jang, H. G.; Sasaki, M.; Jin, S.; Schenkein, D. P.; Su, S. M.; Dang, L.; Fantin, V. R.; Mak, T. W. *J. Exp. Med.* **2010**, *207*, 339-344.
(17) Xu, W. et al. *Cancer Cell* **2011**, *19*, 17-30.
(18) Evangelio, E.; Rath, N. P.; Mirica, L. M. *Dalton Trans.* **2012**, *41*, 8010-8021.

Appendices

Liviu M. Mirica

Washington University
Department of Chemistry, Campus Box 1134
One Brookings Drive,
St. Louis, MO 63130-4899

Phone: (314) 935-3464
Fax: (314) 935-4481
Email: mirica@wustl.edu
Webpage: www.chemistry.wustl.edu/faculty/mirica

PROFESSIONAL POSITIONS

2011-present Member, International Center for Advanced Renewable Energy & Sustainability (I-CARES), Washington University

2008-present Member, Division of Biological and Biomedical Sciences (DBBS), Washington University

2008-present Assistant Professor, Department of Chemistry, Washington University

2005-2008 NIH Postdoctoral Fellow, University of California, Berkeley

Postdoctoral Advisor: *Professor Judith P. Klinman*

EDUCATION

1999–2005 Ph.D., Chemistry, Stanford University, Stanford, CA

Thesis title: "Mechanistic Investigations of Model Complexes Relevant to Copper-Containing Enzymes." Graduate Advisor: *Professor T. Daniel P. Stack*

1996–1999 B.S., Chemistry, California Institute of Technology, Pasadena, CA

Undergraduate Research Advisor: *Professor Harry B. Gray*

AWARDS AND HONORS

- Undergraduate Research Mentor of the Year Award, Washington University, 2012
- Alfred P. Sloan Foundation Research Fellowship, 2012
- Outstanding Faculty Member Nomination, Freshman Class Council & First Year Center, 2011
- Sony Electronics Scholarship Award for Excellence in Teaching, Washington University, 2011
- Ralph E. Powe Junior Faculty Award, Oak Ridge Associated Universities, 2010-2011
- Doctoral New Investigator, Petroleum Research Fund, American Chemical Society, 2009-2011
- NIH–NRSA Postdoctoral Fellowship, 2007-2008

- Young Investigator Award, Division of Inorganic Chemistry, ACS, 2006
- Franklin Veatch Memorial Fellowship, Stanford University, 2004-2005
- Stanford Graduate Fellowship, Stanford University, 1999-2003
- Taube Prize, Stanford University, 1999
- Merck Index Award for Excellence in Chemistry, California Institute of Technology, 1999
- Carnation Merit Award, California Institute of Technology, 1997-1998
- Silver Medal, International Chemistry Olympiad, Beijing, China, 1995
- Gold Medal, International Chemistry Olympiad, Oslo, Norway, 1994

RESEARCH INTERESTS

Design, synthesis, and characterization of novel transition metal complexes that can mediate redox processes relevant to energy applications and oxidative organic transformations. Targeted reactions include: a) the aerobic oxidative oligomerization of hydrocarbons catalyzed by high-valent late transition metal complexes, relevant to the conversion of natural gas into liquid fuels; b) novel catalytic oxidative C-H functionalization reactions using green oxidants such as O_2; and c) the electrocatalytic reduction of carbon dioxide using low-valent late transition metal complexes, aimed at the conversion of CO_2 into useful chemicals.

Bioinorganic projects include: a) studying the role of transition metal ions in amyloid β (Aβ) peptide aggregation in Alzheimer's Disease (AD) and development of metal-binding bifunctional compounds as potential therapeutic and diagnostic agents for AD; and b) the development of specific inhibitors for iron-dependent histone demethylases, a new class of enzymes that play an important role in transcription regulation.

RESEARCH SUPPORT

Current Support

- **American Chemical Society**, Petroleum Research Fund, New Directions Research Grant, "Aerobic Oxidative C-C and C-heteroatom Bond Formation Reactions Catalyzed by Novel Pd(III) and Pd(IV) Complexes", $100,000 direct costs, 03/01/13 – 02/28/15, PI: Mirica.
- **Alfred P. Sloan Foundation**, 2012 Alfred P. Sloan Research Fellowship, $50,000 direct costs, 09/15/2012 – 08/14/2014, PI: Mirica.
- **Department of Energy**, Office of Basic Sciences, Catalysis Science Program, "Novel Palladium Catalysts for the Aerobic Oxidative Oligomerization of Methane & Carbon Dioxide Reduction", $450,000 total costs, 09/15/2011 – 09/14/2014, PI: Mirica.

- **I-CARES Pilot Program**, Washington University in St. Louis, "Novel Catalysts for the Conversion of Methane and Carbon Dioxide into Liquid Fuels", $36,000 direct costs, 05/01/2011 – 04/30/2013, PI: Mirica, co-PI's: Sophia Hayes (WU Chemistry) and Mark Conradi (WU Physics).

Pending Support

- **National Science Foundation**, "CAREER: Oxidative Reactivity of Pd and Ni Complexes Employing Paramagnetic Oxidation States", $610,101 total costs, 06/01/2013 – 05/31/2018, PI: Mirica.
- **Alzheimer's Association**, New Investigator Research Grant, "Novel Chemical Agents as Theranostic Tools for Soluble Aβ Oligomer Aggregation", $100,000 direct costs, 04/01/13 – 03/31/15, PI: Mirica.

Completed Support

- **American Chemical Society**, Petroleum Research Fund, "Study of Water Oxidation by Binuclear Metal Complexes", $100,000 direct costs, 10/01/2009 – 08/31/2011, PI: Mirica
- **Oak Ridge Associated Universities**, Ralph E. Powe Junior Faculty Award, "Novel Imaging Agents for Early Diagnosis of Alzheimer's Disease.", $10,000 direct costs, 06/01/2010 – 05/31/2011, PI: Mirica
- **Washington University Alzheimer's Disease Research Center**, Pilot Research Grant, part of NIA-NIH grant P41RR000954, "Novel Bifunctional Metal Chelators as Selective Binders to Soluble Aβ Oligomers", $35,000 direct costs, 05/01/2011 – 04/30/2012, PI: Mirica.
- **Department of Defense**, Breast Cancer Research Program Concept Award, "Specific Inhibitors of Histone Demethylases: Novel Chemical Agents for Breast Cancer Therapy", $113,802 total costs, 08/01/2010 – 07/31/2012, PI: Mirica

Planned Submissions (near term)

- **National Institutes of Health**, National Institute of Aging, "Novel Theranostic Agents for Soluble Aβ Oligomer Aggregation in Alzheimer's Disease", to be submitted in February 2013, PI: Mirica.
- **National Institutes of Health**, National Institute of General Medical Sciences, "Histone Demethylases in Epigenetic Control: Functional Studies and Specific Inhibitor Development", to be submitted in February 2013, PI: Mirica.

PUBLICATIONS (* denotes corresponding author)

Submitted Manuscripts

32. Sharma, A. K.; Pavlova, S. T.; Kim, J.; Zhang, Y.; Kim, J.; Mirica, L. M.* "The Effect of Cu^{2+} and Zn^{2+} on $A\beta_{42}$ Aggregation and Implications for Cellular Toxicity", submitted to *Inorg. Chem.*

31. Khusnutdinova, J. R.; Rath, N. P.; Mirica, L. M.* "Late First Row Transition Metal Complexes Supported by a Tetradentate Pyridinophane Ligand: Electronic Properties and Reactivity Implications", submitted to *Inorg. Chem.*

30. Luo, J.; Rath, N. P.; Mirica, L. M.* "Oxidative Reactivity of (N2S2)PdRX Complexes (R = Me, Cl; X = Me, Cl, Br): Formation of Pd(III) and Pd(IV) Intermediates", submitted to *Organometallics*.

Published Articles

29. Cascella, B.; Mirica, L. M.* "Kinetic Analysis of Iron-Dependent Histone Demethylases: α-Ketoglutarate Substrate Inhibition and Potential Relevance to the Regulation of Histone Demethylation in Cancer Cells", *Biochemistry*, **2012**, *51*, 8699-8701, DOI: 10.1021/bi3012466.

28. Tang, F.; Qu, F.; Khusnutdinova, J. R.; Rath, N. P.; Mirica, L. M.* "Structural and Reactivity Comparison of Analogous Organometallic Pd(III) and Pd(IV) Complexes", *Dalton Trans.*, **2012**, *41*, 14046-14050, DOI:10.1039/C2DT32127K.

27. Tang, F.; Zhang, Y.; Rath, N. P.; Mirica, L. M.* "Detection of Pd(III) and Pd(IV) Intermediates during the Aerobic Oxidative C-C Bond Formation from a Pd(II) Dimethyl Complex", *Organometallics*, **2012**, *31*, 6690-6696. DOI: 10.1021/om300752w.

26. Khusnutdinova, J. R.; Mirica, L. M.* "Organometallic Pd(III) Complexes in C-C and C-Heteroatom Bond Formation Reactions", invited book chapter in *C-H Activation and Functionalization, Transition Metal Mediation*, Royal Society of Chemistry, 2012, in press.

25. Khusnutdinova, J. R.; Qu, F.; Zhang, Y.; Rath, N. P.; Mirica, L. M.* "Formation of the Pd(IV) Complex $[(Me_3tacn)Pd^{IV}Me_3]^+$ through Aerobic Oxidation of $(Me_3tacn)Pd^{II}Me_2$ (Me_3tacn = N,N',N''-trimethyl-1,4,7-triazacyclononane)", *Organometallics*, **2012**, *31*, 4627-4630, DOI: 10.1021/om300426r. Featured on the cover of issue 13.

24. Mirica, L. M.;* Khusnutdinova, J. R., "Structure and Electronic Properties of Pd(III) Complexes", *Coord. Chem. Rev.*, **2012**, *256*, DOI: 10.1016/j.ccr.2012.04.030.

23. Evangelio, E.; Rath, N. P.; Mirica, L. M.* "Cycloaddition Reactivity Studies of First Row Transition Metal-Azide Complexes and Alkynes: An Inorganic Click Reaction for

Metalloenzyme Inhibitor Synthesis", *Dalton Trans.*, **2012**, *41*, 8010-8021, DOI: 10.1039/C2DT30145H. Invited contribution for the "New Talent Americas" issue.

22. Sharma, A. K.; Pavlova, S. T.; Kim, J.; Finkelstein, D.; Hawco, N. J.; Rath, N. P.; Kim, J.; Mirica, L. M.* "Bifunctional Metal-Binding Compounds for Controlling the Metal-Mediated Aggregation of the Aβ42 Peptide", *J. Am. Chem. Soc.*, **2012**, *134*, 6625-6636, DOI: 10.1021/ja210588m.

21. Khusnutdinova, J. R.; Rath, N. P.; Mirica, L. M.* "The Aerobic Oxidation of a Pd(II) Dimethyl Complex Leads to Selective Ethane Elimination from a Pd(III) Intermediate", *J. Am. Chem. Soc.*, **2012**, *134*, 2414-2422, DOI: 10.1021/ja210841f.

20. Luo, J.; Khusnutdinova, J. R.; Rath, N. P.; Mirica, L. M.* "Unsupported d^8-d^8 Interactions in Cationic Pd^{II} and Pt^{II} Complexes: Evidence for a Significant Metal-Metal Bonding Character", *Chem. Comm.*, ***2012***, *48*, 1532-1534, DOI: 10.1039/C1CC15420F. Invited contribution for the "Emerging Investigators" issue.

19. Luo, J.; Rath, N. P.; Mirica, L. M.* "Dinuclear Co(II)Co(III) Mixed-Valence and Co(III)Co(III) Complexes with N- and O-Donor Ligands: Characterization and Water Oxidation Studies", *Inorg. Chem.*, **2011**, *50*, 6152-6157, DOI: 10.1021/ic201031s.

18. Khusnutdinova, J. R.; Rath, N. P.; Mirica, L. M.* "Dinuclear Pd(III) Complexes with a Single Unsupported Bridging Halide Ligand: Reversible Formation from Mononuclear Pd(II) or Pd(IV) Precursors", *Angew. Chem. Int.Ed.*, **2011**, *50*, 5532-5536, DOI: 10.1002/anie.201100928.

17. Khusnutdinova, J. R.; Rath, N. P.; Mirica, L. M.* "Stable Mononuclear Organometallic Pd(III) Complexes and Their C-C Bond Formation Reactivity", *J. Am. Chem. Soc.*, **2010**, *132*, 7303-7305; DOI: 10.1021/ja103001g. Featured as "News of the Week" in *Chem. & Eng. News*, **2010**, *88*, 21, 9.

Publications from Postdoctoral and Ph.D. Studies

16. Verma, P.; Weir, J.; Mirica, L. M.; Stack, T. D. P.* "Tale of a Twist: Magnetic and Optical Switching in Copper(II) Semiquinone Complexes", *Inorg. Chem.*, **2011**, *50*, 9816-9825.

15. Op't Holt, B. T.; Vance, M. A.; Mirica, L. M.; Heppner, D. E.; Stack, T. D. P.,* Solomon E. I.* "Reaction Coordinate of a Functional Model of Tyrosinase: Spectroscopic and Computational Characterization", *J. Am. Chem. Soc.*, **2009**, *131*, 6421-6438.

14. Humphreys, K. J.; Mirica, L. M.; Wang Y.; Klinman, J. P.* "Galactose Oxidase as a Model for Reactivity at a Copper Superoxide Center", *J. Am. Chem. Soc.*, **2009**, *131*, 4657-4663.

13. Mirica, L. M.; McCusker, K. P.; Munos, J. W.; Liu, H. W.; Klinman, J. P.* "Probing the Nature of Reactive Fe/O_2 Intermediates in Non-Heme Iron Enzymes through ^{18}O Kinetic Isotope Effects", *J. Am. Chem. Soc.*, **2008**, *130*, 8122-8123.

12. Mirica, L. M.; Klinman, J. P.* "The Nature of O_2 Activation by the Ethylene-Forming Enzyme ACC Oxidase", *Proc. Natl. Acad. Sci. U. S. A.*, **2008**, *105*, 1814-1819.

11. Welford, R. W. D.; Lam, A.; Mirica, L. M.; Klinman, J. P.* "Partial Conversion of *Hansenula polymorpha* Amine Oxidase into a 'Plant' Amine Oxidase: Implications for Copper Chemistry and Mechanism", *Biochemistry*, **2007**, *46*, 10817-10827.

10. Thrower, J. T.; Mirica, L. M.; McCusker, K. P.; Klinman, J. P.* "Mechanistic Investigations of 1-Aminocylcyclopropane 1-Carboxylic Acid Oxidase with Alternate Cyclic and Acyclic Substrates", *Biochemistry*, **2006**, *45*, 13108-13117.

9. Mirica, L. M.; Rudd, D. J.; Vance, M.; Solomon, E. I.;* Hedman, B.;* Hodgson, K. O.;* Stack, T. D. P.* "A μ-η^2:η^2-Peroxodicopper(II) Complex with a Secondary Diamine Ligand: A Functional Model of Tyrosinase", *J. Am. Chem. Soc.*, **2006**, *128*, 2654-2665.

8. Cole, A. P.; Mahadevan, V.; Mirica, L. M.; Ottenwaelder, X.; Stack, T. D. P.* "Bis(μ-oxo)dicopper(III) Complexes of a Homologous Series of Simple Peralkylated 1,2-Diamines: Steric Modulation of Structure, Stability, and Reactivity", *Inorg. Chem.*, **2005**, *44*, 7345-7364.

7. Yoon, J.; Mirica, L. M.; Stack, T. D. P.;* Solomon, E. I.* "Variable-Temperature Variable-Field Magnetic Circular Dichroism Studies of Tris-Hydroxy and μ_3-Oxo Bridged Trinuclear Cu(II) Complexes: Geometric and Electronic Structures of the Native Intermediate of Multicopper Oxidases", *J. Am. Chem. Soc.*, **2005**, *127*, 13680-13693.

6. Mirica, L. M.; Vance, M.; Rudd, D. J.; Hedman, B.;* Hodgson, K. O.;* Solomon, E. I.;* Stack, T. D. P.* "Tyrosinase Reactivity in a Model Complex: An Alternative Hydroxylation Mechanism", *Science*, **2005**, *308*, 1890-1892. Featured as a perspective in *Science*, **2005**, *308*, 1876-1877 and a science concentrate in *Chem. & Eng. News*, **2005**, *83*, 26, 38.

5. Mirica, L. M.; Stack, T. D. P. * "A Tris(μ-hydroxy)tricopper(II) Complex as a Model of the Native Intermediate in Laccase and Its Relationship to a Binuclear Analogue", *Inorg. Chem.*, **2005**, *44*, 2131-2133.

4. Pratt, R. C.; Mirica, L. M.; Stack, T. D. P.* "Snapshots of a Metamorphosing Cu(II) Ground State in a Galactose Oxidase-Inspired Complex", *Inorg. Chem.*, **2004**, *43*, 8030-8039.

3. Yoon, J.; Mirica, L. M.; Stack, T. D. P.;* Solomon, E. I.* "Spectroscopic Demonstration of a Large Antisymmetric Exchange Contribution to the Spin-Frustrated Ground State of a D_3 Symmetric Hydroxy-Bridged Trinuclear Cu(II) Complex: Ground-to-Excited State Superexchange Pathways", *J. Am. Chem. Soc.*, **2004**, *126*, 12586-12595.

2. Mirica, L. M.; Ottenwaelder, X.; Stack, T. D. P.* "Structure and Spectroscopy of Copper–Dioxygen Complexes", *Chem. Rev.*, **2004**, *104*, 1013-1046.

1. Mirica, L. M.; Vance, M.; Rudd, D. J.; Hedman, B.;* Hodgson, K. O.;* Solomon, E. I.;* Stack, T. D. P.* "A Stabilized μ-η^2:η^2-Peroxodicopper(II) Complex with a Secondary

Diamine Ligand and Its Tyrosinase-like Reactivity", *J. Am. Chem. Soc.* **2002**, *124*, 9332-9333.

INVITED PRESENTATIONS

48. "Organometallic Reactivity of High-Valent Pd and Ni Complexes Supported by Tetradentate and Tridentate Ligands", invited talk, *Organometallics Gordon Research Conference*, July 2013.
47. "Oxidative Reactivity of High-Valent Pd Complexes Supported by Flexible Multidentate Ligands", symposium talk, *American Chemical Society National Meeting*, New Orleans, April 2013.
46. "Aerobic Oxidative C-C and C-Heteroatom Bond Formation Reactions Involving High-Valent Pd Intermediates", Department of Chemistry, *Johns Hopkins University,* April 2013.
45. "Aerobic Oxidative C-C and C-Heteroatom Bond Formation Reactions Involving High-Valent Pd Intermediates", Department of Chemistry, *Georgetown University,* April 2013.
44. "Aerobic Oxidative C-C and C-Heteroatom Bond Formation Reactions Involving High-Valent Pd Intermediates", Department of Chemistry, *University of Maryland,* April 2013.
43. "Aerobic Oxidative C-C and C-Heteroatom Bond Formation Reactions Involving High-Valent Pd Intermediates", Department of Chemistry, *MIT,* March 2013.
42. "Aerobic Oxidative C-C and C-Heteroatom Bond Formation Reactions Involving High-Valent Pd Intermediates", Department of Chemistry, *Harvard University,* March 2013.
41. "Aerobic Oxidative C-C and C-Heteroatom Bond Formation Reactions Involving High-Valent Pd Intermediates", Department of Chemistry, *University of California, Santa Barbara,* March 2013.
40. "Aerobic Oxidative C-C and C-Heteroatom Bond Formation Reactions Involving High-Valent Pd Intermediates", Department of Chemistry, *University of California, San Diego,* March 2013.
39. "Aerobic Oxidative C-C and C-Heteroatom Bond Formation Reactions Involving High-Valent Pd Intermediates", Department of Chemistry, *University of California, Los Angeles,* February 2013.
38. "Aerobic Oxidative C-C and C-Heteroatom Bond Formation Reactions Involving High-Valent Pd Intermediates", Department of Chemistry, *University of Southern California,* February 2013.
37. "Aerobic Oxidative C-C and C-Heteroatom Bond Formation Reactions Involving High-Valent Pd Intermediates", Department of Chemistry, *Caltech*, February 2013.

36. "Aerobic Oxidative C-C and C-Heteroatom Bond Formation Reactions Involving High-Valent Pd Intermediates", Department of Chemistry, *University of California, Berkeley,* February 2013.

35. "Aerobic Oxidative C-C and C-Heteroatom Bond Formation Reactions Involving High-Valent Pd Intermediates", Department of Chemistry, *Stanford University,* February 2013.

34. "Aerobic Oxidative C-C and C-Heteroatom Bond Formation Reactions Involving High-Valent Pd Intermediates", Department of Chemistry, *University of Florida,* February 2013.

33. "Aerobic Oxidative C-C and C-Heteroatom Bond Formation Reactions Involving High-Valent Pd Intermediates", Department of Chemistry, *North Carolina State University,* February 2013.

32. "Aerobic Oxidative C-C and C-Heteroatom Bond Formation Reactions Involving High-Valent Pd Intermediates", Department of Chemistry, *University of North Carolina, Chapel Hill,* January 2013.

31. "Aerobic Oxidative C-C and C-Heteroatom Bond Formation Reactions Involving High-Valent Pd Intermediates", Department of Chemistry, *Texas A&M University,* November 2012.

30. "Aerobic Oxidative C-C and C-Heteroatom Bond Formation Reactions Involving High-Valent Pd Intermediates", Department of Chemistry, *Yale University,* November 2012.

29. "Aerobic Oxidative C-C and C-Heteroatom Bond Formation Reactions Involving High-Valent Pd Intermediates", Department of Chemistry, *Indiana University,* November 2012.

28. "The Importance of Undergraduate Research in My Academic Career", keynote speaker, Undergraduate Research Symposium, Washington University, October, 2012.

27. "Aerobic Oxidative C-C and C-Heteroatom Bond Formation Reactions Involving High-Valent Pd Intermediates", Department of Chemistry, *University of Wisconsin, Madison,* October 2012.

26. "Aerobic Oxidative C-C and C-Heteroatom Bond Formation Reactions Involving High-Valent Pd Intermediates", Department of Chemistry, *University of Delaware,* October 2012.

25. "Stable Mononuclear Pd(III) and Pd(IV) Complexes: Reactivity Comparison and Relevance to Aerobic C-C Bond Formation", *NSF Workshop on Synthesis*, MIT Endicott House, Dedham, MA, May 2012.

24. "Stable Pd(III) and Pd(IV) Complexes Supported by Tetradentate and Tridentate Ligands and Their C-C Bond Formation Reactivity", *Mesilla Chemistry Workshop*, Las Cruces, New Mexico, February 2012.

23. "Stable Pd(III) and Pd(IV) Complexes Supported by Tetradentate and Tridentate Ligands and Their C-C Bond Formation Reactivity", Department of Chemistry, *University of California, Irvine*, December 2011.

22. "The Reaactivity of Stable Pd(III) and Pd(IV) Complexes Supported by Tetradentate and Tridentate Ligands", *Zing Coordination Chemistry Conference*, Mexico, December 2011.

21. "Stable Pd(III) and Pd(IV) Complexes Supported by Tetradentate and Tridentate Ligands and Their C-C Bond Formation Reactivity", Department of Chemistry, *University of Michigan, Ann Arbor*, November 2011.

20. "Late Transition Metal Catalysts for the Activation of Small Molecules: Relevance to Renewable Energy Catalysis", Department of Chemistry, *University of Louisville*, November 2011.

19. "Stable Pd(III) and Pd(IV) Complexes Supported by Tetradentate and Tridentate Ligands and Their C-C Bond Formation Reactivity", Department of Chemistry, *University of Missouri, Columbia*, October 2011.

18. "Late Transition Metal Catalysts for the Activation of Small Molecules: Relevance to Renewable Energy Catalysis", Department of Chemistry, *Missouri State University*, October 2011.

17. "Late Transition Metal Catalysts for the Activation of Small Molecules: Relevance to Renewable Energy Catalysis", Department of Chemistry, *Macalester College*, September 2011.

16. "Late Transition Metal Catalysts for the Activation of Small Molecules: Relevance to Renewable Energy Catalysis", Department of Chemistry, *Western Michigan University*, September 2011.

15. "New Chemical Agents for Controlling Amyloid β Peptide Aggregation in Alzheimer's Disease", *International Conference on Biological Inorganic Chemistry (ICBIC15)*, Vancouver, August 2011.

14. "Late Transition Metal Catalysts for the Activation of Small Molecules: Relevance to Renewable Energy Catalysis", *Challenges in Renewable Energy – International Symposia on Advancing the Chemical Sciences (ISACS4)*, MIT, Boston, July 2011.

13. "New Chemical Agents for Controlling Histone Demethylation and Amyloid β Peptide Aggregation", Department of Biochemistry and Molecular Biophysics, *Washington University School of Medicine*, April 2011.

12. "Late Transition Metal Catalysts for the Activation of Small Molecules: Relevance to Renewable Energy Catalysis", Department of Chemistry, *Saint Louis University*, February 2011.

11. "Late Transition Metal Catalysts for the Activation of Small Molecules: Relevance to Renewable Energy Catalysis", Department of Chemistry, *Southern Illinois University - Edwardsville*, January 2011.

10. "New Chemical Agents for Controlling Amyloid β Peptide Aggregation in Alzheimer's Disease", Alzheimer's Disease Research Center, *Washington University School of Medicine*, December 2010.

9. "Late Transition Metal Catalysts for the Activation of Small Molecules: Relevance to Renewable Energy Catalysis", *Midstates Consortium Undergraduate Research Symposium*, Washington University in St. Louis, November 2010.

8. "Stable Mononuclear Organometallic Pd(III) Complexes and Their C-C Bond Formation Reactivity", *Missouri Inorganic Day*, Saint Louis University, May 2010.

7. "Renewable Energy Catalysis: Studies of Water Oxidation by Bimetallic Complexes", Department of Chemistry and Biochemistry, *University of Missouri – St. Louis*, April 2010.

6. *"*Development of Specific Inhibitors for Histone Demethylases*", NIH Mentoring Workshop for Junior Faculty*, University of California, Irvine, October 2009.

5. "New Chemical Agents for Imaging and Controlling Amyloid β Peptide Aggregation in Alzheimer's Disease", Department of Radiology, *Washington University School of Medicine*, September 2009.

4. "Renewable Energy Catalysis: Studies of Water Oxidation by Bimetallic Complexes", Department of Chemistry, Departmental seminar and recruiting visit, *Illinois State University*, April 2009.

3. "Mechanistic Studies of the Ethylene-forming Enzyme ACC Oxidase", *13th International Conference on Biological Inorganic Chemistry*, Vienna, Austria, July 2007.

2. "Tyrosinase Reactivity in a Model Complex: An Alternative Hydroxylation Mechanism", Young Investigator Symposium, *232nd National Meeting of the American Chemical Society*, San Francisco, September 2006.

1. "Phenolate Hydroxylation Reactivity of a μ-η^2:η^2-Peroxodicopper(II) Complex: Peroxide O–O Bond Cleavage Precedes C–O Bond Formation", *Gordon Graduate Research Seminar: Bioinorganic Chemistry*, Ventura, January 2005.

CONTRIBUTED PRESENTATIONS (presenting author is underlined)

28. Tang F.; Qu F.; Khusnutdinova J. R.; Rath N. P.; Mirica L. M.* "Stable Pd(III) and Pd(IV) Complexes Supported by Tetradentate and Tridentate Ligands and Their C-C Bond Formation Reactivity", poster talk, *Organometallics Gordon Research Conference*, July 2012.

27. Sharma, A. K.; Mirica, L. M.* "Bifunctional Compounds for Controlling Metal-Mediated Aggregation of the Aβ42 Peptide", oral presentation, *Missouri Inorganic Day*, University of Missouri – St. Louis, May 2012.

26. Qu, F.; Khusnutdinova, J. R.; Rath, N. P.; Mirica, L. M.* *"*Stable Mononuclear (^{iPr}N4)Pd(III) and Pd(IV) Complexes: Characterization and Reactivity Studies*"*, oral presentation, *Missouri Inorganic Day*, University of Missouri – St. Louis, May 2012.

25. Tang, Q.; Khusnutdinova, J. R.; Rath, N. P.; Mirica, L. M.* *"*Stable mononuclear Pd(III) and Pd(IV) complexes in identical ligand environment: Characterization and direct reactivity comparison*"*, oral presentation, *46th Midwest Regional Meeting of the American Chemical Society*, St. Louis, October 2011.

24. Luo, J.; Rath, N. P.; Mirica, L. M.* *"*Dinuclear Pd^{II} and Pt^{II} complexes with unsupported d^8-d^8 interactions*"*, oral presentation, Oral presentation, *46th Midwest Regional Meeting of the American Chemical Society*, St. Louis, October 2011.

23. Qu, F.; Khusnutdinova, J. R.; Rath, N. P.; Mirica, L. M.* *"*New (^{iPr}N4)Pd^{III} and (^{iPr}N4)Pd^{IV} Complexes*"*, oral presentation, *46th Midwest Regional Meeting of the American Chemical Society*, St. Louis, October 2011.

22. Park. S.; Tang, Q.; Mirica, L. M.* *"*Synthesis and Electrochemical Properties of Various Pd(II) Complexes*"*, poster presentation, *46th Midwest Regional Meeting of the American Chemical Society*, St. Louis, October 2011.

21. Zhang, Y.; Mirica, L. M.;* Gross, M. L.* *"*H/DX-Mass Spectrometry Study of the beta-Amyloid (Ab1-42) Peptide Oligomer*"*, poster presentation, *46th Midwest Regional Meeting of the American Chemical Society*, St. Louis, October 2011.

20. Cascella, B.; Mirica L. M.* *"*Development of Specific Inhibitors for JmjC-Domain Histone Demethylases*"*, poster presentation, *46th Midwest Regional Meeting of the American Chemical Society*, St. Louis, October 2011.

19. Cascella, B.; Mirica L. M.* *"*Development of Specific Inhibitors for Histone Demethylases*"*, poster presentation, *Era of HOPE* conference, DOD CMDRP program, Orlando, Florida, August 2011.

18. Tang, Q.; Mirica L. M.* *"*Stable mononuclear Pd(III) and Pd(IV) complexes in identical ligand environment: Characterization and direct reactivity comparison*"*, oral presentation, *Missouri Inorganic Day*, Missouri State University, May 2011.

17. Luo, J.; Mirica L. M.* *"*Dinuclear Pd^{II} and Pt^{II} complexes with unsupported d^8-d^8 interactions*"*, oral presentation, *Missouri Inorganic Day*, Missouri State University, May 2011.

16. Khusnutdinova, J. R.; Rath N. P.; Mirica L. M.* *"*Mononuclear alkyl and aryl Pd(III) complexes and their reactivity in C-C and C-X bond formation*"*, oral presentation and session chair, *American Chemical Society National Meeting*, Boston, August 2010.

15. Khusnutdinova, J. R.; Rath N. P.; Mirica L. M.* *"*Synthesis, characterization and electrochemical studies of Pd(III) complexes stabilized by polydentate N-donor ligands*"*, oral presentation, *American Chemical Society National Meeting*, Boston, August 2010.

14. Tang, Q.; Mirica L. M.* *"*Binucleating ligands: Control of the M-M distance in transition metal complexes*"*, oral presentation, *American Chemical Society National Meeting*, Boston, August 2010.

13. Luo, J.; Mirica L. M.* *"*Synthesis, electrochemistry, and magnetic properties of a binuclear bis(μ-OMe) Co(II)Co(III) mixed-valent complex*"*, oral presentation, *American Chemical Society National Meeting*, Boston, August 2010.

12. Hawco, N. J.; Mirica L. M.* *"*Aggregation studies of amyloid beta peptide in the presence of metal cations and metal binding-compounds*"*, poster presentation, *American Chemical Society National Meeting*, Boston, August 2010.

11. Khusnutdinova, J. R.; Rath N. P.; Mirica L. M.* *"*Stable Mononuclear Organometallic Pd(III) Complexes and Their C-C Bond Formation Reactivity*"*, poster talk, *Organometallics Gordon Research Conference*, July 2010.

10. Khusnutdinova, J. R.; Rath N. P.; Mirica L. M.* *"*Electrochemical Studies of Pd(II) and Pd(III) Complexes Stabilized by Polydentate N-donor ligands*"*, poster presentation, *Organometallics Gordon Research Conference*, July 2010.

9. Khusnutdinova, J. R.; Rath N. P.; Mirica L. M.* *"*Stable Mononuclear Organometallic Pd(III) Complexes and Their C-C Bond Formation Reactivity*"*, poster talk, *Inorganic Chemistry Gordon Research Conference*, June 2010.

8. Khusnutdinova, J. R.; Rath N. P.; Mirica L. M.* *"*Stable Mononuclear Organometallic Pd(III) Complexes and Their C-C Bond Formation Reactivity*"*, poster presentation, *Department of Energy, Chemical Catalysis Meeting*, June 2010.

7. Mirica L. M.* *"*Development of Specific Inhibitors for Histone Demethylases*"*, poster presentation and session chair, *Enzymes, Coenzymes & Metabolic Pathways Gordon Research Conference*, Waterville Valley, July 2009.

6. Mirica L. M.* "Renewable Energy Catalysis: Studies of Water Oxidation by Binuclear Metal Complexes", poster presentation, *Renewable Energy: Solar Fuels Gordon Research Conference*, Ventura, February 2009.

5. Mirica L. M.; Klinman J. P.* "The Nature of O_2 Activation by the Ethylene-Forming Enzyme ACC Oxidase", poster presentation, *Metals in Biology Gordon Research Conference*, Ventura, January 2008.

4. Mirica, L. M.; Stack, T. D. P.* "Interconversion of μ-η^2:η^2-Peroxodicopper(II) and Bis(μ-oxo)dicopper(III) Complexes: A Theoretical Study", poster presentation, *12th International Conference on Biological Inorganic Chemistry*, Ann Arbor, Michigan, August 2005.

3. Mirica, L. M.; Vance, M.; Rudd, D. J.; Hedman, B.;* Hodgson, K. O.;* Solomon, E. I.;* Stack, T. D. P.* "Investigation of Tyrosinase-like Reactivity for a Cu/O_2 complex: Insights into the Phenol Hydroxylation Mechanism", oral presentation, *227th National Meeting of the American Chemical Society*, Anaheim, March 2004.

2. Mirica, L. M.; Stack, T. D. P.* "Detection and Characterization of Intermediates during the Hydroxylation of Phenols by a μ-η^2:η^2-Peroxodicopper(II) Complex", poster presentation, *Gordon Graduate Research Seminar: Bioinorganic Chemistry*, Ventura, January 2004.

1. Mirica, L. M.; Stack, T. D. P.* "Synthesis, Characterization, and Reactivity of a New μ-η^2:η^2-Peroxodicopper(II) Complex", oral presentation, *224th National Meeting of the American Chemical Society*, Boston, August 2002.

SYNERGISTIC ACTIVITIES

- Reviewer for *Journal of the American Chemical Society*, *Proceedings of the National Academy of Sciences U.S.A., Accounts of Chemical Research, Inorganic Chemistry*, *Chemistry of Materials*, *Dalton Transactions, Organometallics, ACS Chemical Neuroscience, Inorganica Chimica Acta, Journal of Biological Inorganic Chemistry,* and *Journal of Inorganic Biochemistry*.
- Grant proposal reviewer for *National Science Foundation, ACS Petroleum Research Fund*, *The Research Corporation,* and *The Alzheimer's Association*.

BIOCHEMISTRY
including biophysical chemistry & molecular biology

Rapid Report

pubs.acs.org/biochemistry

Kinetic Analysis of Iron-Dependent Histone Demethylases: α-Ketoglutarate Substrate Inhibition and Potential Relevance to the Regulation of Histone Demethylation in Cancer Cells

Barbara Cascella and Liviu M. Mirica*

Department of Chemistry, Washington University, One Brookings Drive, St. Louis, Missouri 63130-4899, United States

Supporting Information

ABSTRACT: The Jumonji C domain-containing histone demethylases (JmjC-HDMs) are α-ketoglutarate (αKG)-dependent, O_2-activating, non-heme iron enzymes that play an important role in epigenetics. Reported herein is a detailed kinetic analysis of three JmjC-HDMs, including the cancer-relevant JMJD2C, that was achieved by employing three enzyme activity assays. A continuous O_2 consumption assay reveals that HDMs have low affinities for O_2, suggesting that these enzymes can act as oxygen sensors in vivo. An interesting case of αKG substrate inhibition was found, and the kinetic data suggest that αKG inhibits JMJD2C competitively with respect to O_2. JMJD2C displays an optimal activity in vitro at αKG concentrations similar to those found in cancer cells, with implications for the regulation of histone demethylation activity in cancer versus normal cells.

Covalent modification of chromatin by histone methylation has wide-ranging effects on nuclear functions, such as transcriptional regulation, genome integrity, and epigenetic inheritance.[1] Until recently, histone methylation was believed to be a static modification; however, the identification of histone demethylase (HDM) enzymes has revealed that this epigenetic mark is dynamically controlled.[2] The Jumonji C domain-containing HDMs (JmjC-HDMs) catalyze the demethylation of methylated lysine residues through a hydroxylation reaction and belong to the large class of α-ketoglutarate (αKG)-dependent, O_2-activating, non-heme iron enzymes.[3] More than a dozen JmjC-HDMs have been reported and shown to exhibit both residue and methylation state specificity.[4] In addition, JmjC-HDMs have been implicated in cancer and stem cell biology. For example, it has recently been shown that PLU-1 is a HDM that plays an important role in the proliferation of breast cancer cells through transcriptional repression of tumor suppressor genes,[5] while the HDM GASC1 (or JMJD2C) was proposed to be linked to stem cell phenotypes in breast cancer.[6] Thus, it is of great interest to design specific inhibitors for the various HDM subfamilies by utilizing the enzymes' substrate specificities.[7] However, there are limited data available on the enzymology of HDMs. In this regard, we have successfully expressed and purified three HDMs, including the cancer-relevant JMJD2C, and obtained a detailed enzyme kinetic analysis by employing three different assays (vide infra). Interestingly, a case of αKG substrate inhibition was observed, which could have important implications for the regulation of HDM activity in cancer biology.

In the lysine demethylation reaction, HDMs hydroxylate the *N*-methyl substrate to a hydroxymethyl group, which is converted nonenzymatically to formaldehyde and the demethylated product (Scheme 1).[2] Our initial kinetic studies focused on JMJD2A, the first HDM with a resolved crystal structure and one that has been used extensively in biochemical studies.[4] The pseudogene-encoded JMJD2E, with a sequence that is >80% similar to that of JMJD2A, has been often employed in enzyme activity studies as it has the highest activity when compared to those of the other members of the JMJD2 subfamily.[7a,b] Finally, JMJD2C is of great interest because of its implications in brain, breast, prostate, and esophageal cancers,[6,8] yet the kinetics of JMJD2C has not been fully investigated to date.[7c−e]

Scheme 1. Histone Demethylation by JmjC-HDMs, Shown for a Trimethyllysine Substrate

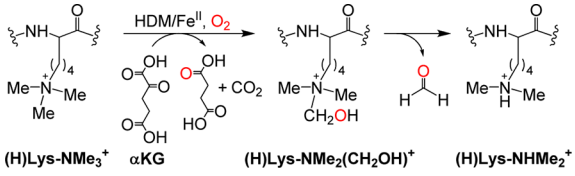

Truncated constructs of JMJD2A,[4b] JMJD2E,[7a] and JMJD2C,[7d] containing the catalytic JmjN and JmjC domains, were transformed into the *Escherichia coli* Rosetta II strain and expressed and purified using published procedures.[9] The enzymatic activity of the three HDMs was monitored by three complementary assays: a coupled formaldehyde dehydrogenase (FDH) NADH fluorescence assay, a discontinuous MALDI-TOF mass spectrometry (MS) assay, and a continuous O_2 consumption assay. Initially, kinetic parameters were obtained using an adapted version of the widely employed FDH-coupled assay,[4c,10] and a trimethylated H3K9me$_3$ octapeptide as the histone substrate analogue.[9] Demethylation of the peptide substrate was also confirmed by MALDI-TOF MS, and quantification of the peptide products was correlated to the extent of demethylation measured using the other enzymatic assays.[9] Since no direct continuous HDM activity

Received: September 14, 2012
Revised: October 13, 2012
Published: October 15, 2012

   dx.doi.org/10.1021/bi3012466 | *Biochemistry* 2012, 51, 8699−8701

Table 1. Kinetic Parameters for the Three JmjC-HDMs, JMJD2A, JMJD2E, and JMJD2C[a]

		H3K9me$_3$	O_2	αKG
HDM	assay	K_m^{app} (μM), k_{cat}^{app} (min^{-1})[b]	K_m^{app} (μM), k_{cat}^{app} (min^{-1})	K_m^{app} (μM), K_i^{app} (mM)[d]
JMJD2A	O_2 consumed	31 ± 3, 2.5 ± 0.1[b]	57 ± 10, 2.5 ± 0.1	10 ± 1, 10 ± 2[d]
	coupled FDH	104 ± 16, 1.4 ± 0.1[b]	NM[c]	21 ± 4, 13 ± 3[d]
JMJD2E	O_2 consumed	38 ± 3, 3.3 ± 0.1[b]	197 ± 16, 4.0 ± 0.1	21 ± 2, 12 ± 1[d]
	coupled FDH	224 ± 15, 2.1 ± 0.1[b]	NM[c]	37 ± 7, 11 ± 3[d]
JMJD2C	O_2 consumed	32 ± 3, 2.1 ± 0.1[b]	158 ± 13, 2.6 ± 0.1	12 ± 2, 4.3 ± 0.6[d]
	coupled FDH	76 ± 11, 0.70 ± 0.03[b]	NM[c]	22 ± 5, 3.4 ± 0.6[d]

[a]See the Supporting Information for assay conditions. [b]k_{cat}^{app} values were determined at 258 μM O_2. [c]Not measured. [d]αKG K_i^{app} values reported at 258 μM O_2.

assay has been developed to date, we have employed for the first time an O_2 consumption assay to measure in real-time the HDM enzymatic activity by using a Clark oxygen electrode.[9,11]

Using the assays described above, we have determined the kinetic parameters for the three JmjC-HDMs with respect to all three substrates: the ARK(me$_3$)STGGK peptide substrate, O_2, and αKG. For JMJD2A and JMJD2C, the FDH-coupled assay yielded K_m values for the peptide substrate (104 ± 16 μM for JMJD2A and 76 ± 11 μM for JMJD2C) that are similar to those found in the literature,[4a,7e,12] while for JMJD2E, a slightly larger K_m value was obtained [224 ± 15 μM (Table 1)].[a] Interestingly, the use of the O_2 consumption assay reveals significantly reduced peptide K_m values for JMJD2A (31 ± 3 μM), JMJD2E (38 ± 3 μM), and JMJD2C (32 ± 3 μM), as well as turnover numbers that are similar or higher than those from other studies.[4a,7e,12] The O_2 consumption assays can be performed under saturating conditions for all substrates and thus provide a unique opportunity to obtain true k_{cat} values for the three HDMs (Table 1). Most importantly, the observed activity of JMJD2C is higher than that reported previously[7e] and comparable to those of JMJD2A and JMJD2E.[7] Thus, JMJD2C can now be used in inhibition studies employing the O_2 consumption assay, especially given its direct implication in cancer biology.[6] Overall, the O_2 consumption assay seems to allow for a superior characterization of HDMs versus the FDH-coupled assay, because the obtained K_m values for the peptide substrate are more in line with the expected affinities for the natural substrate in vivo, while higher turnover numbers were also found for all three HDMs investigated.[9]

Using the O_2 consumption assay, we have measured for the first time the $K_m(O_2)$ values for HDMs and found that these enzymes have relatively low apparent affinities for O_2, with K_m values near or above the normal cellular O_2 concentration [57 ± 10 μM for JMJD2A, 197 ± 16 μM for JMJD2E, and 158 ± 13 μM for JMJD2C (Figure 1)].[13] Such O_2 affinities suggest the enzymatic activity can be altered by small changes in O_2 concentration, and thus, the JmjC-HDMs can act as oxygen sensors in vivo, as observed previously for other αKG-dependent non-heme iron oxygenases involved in the hypoxic response.[13] In contrast, the enzymes' affinities for αKG are high compared to those for O_2, and in line with values reported previously.[7a,14] For all three HDMs investigated, the αKG K_m values are between 10 and 37 μM and differ by <2-fold between the FDH-coupled assay and the O_2 consumption assay, with the latter technique providing slightly lower K_m values (Table 1).

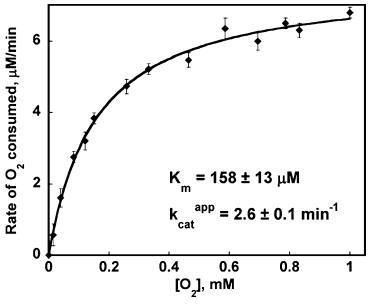

Figure 1. Michaelis–Menten plot for JMJD2C obtained using a Clark oxygen electrode and varying O_2 concentrations.[9]

Interestingly, we found a mild αKG substrate inhibition effect for JMJD2A and JMJD2E when αKG was present in high concentrations (>1 mM).[9] The apparent K_i values were obtained using the FDH-coupled assay (for JMJD2A, K_i^{app} = 13 ± 3 mM; for JMJD2E, K_i^{app} = 11 ± 3 mM) and the O_2 consumption assay [for JMJD2A, K_i^{app} = 10 ± 2 mM; for JMJD2E, K_i^{app} = 12 ± 1 mM (Table 1)]. Interestingly, the αKG inhibitory effect is significantly stronger in the case of JMJD2C [with the FDH-coupled assay, K_i^{app} = 3.4 ± 0.6 mM (Figure 2);

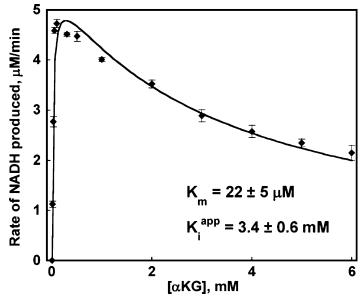

Figure 2. Inhibition of JMJD2C by αKG, measured by the FDH-coupled assay.[9]

with the O_2 electrode assay, K_i^{app} = 4.3 ± 0.6 mM (Figure S5 of the Supporting Information)]. Although previous studies reported the inhibition of other αKG-dependent Fe(II) oxygenases by αKG,[15] the type of inhibition with respect to the other substrates was not investigated in detail. In this regard, the inhibition of JMJD2C by αKG was measured at constant αKG concentrations (300 μM, 2 mM, 4 mM, and 5 mM) and variable O_2 concentrations. It was found that the K_m value for O_2 increased with an increasing αKG concentration, while the V_{max} value stayed relatively constant (Figure S8 of the Supporting Information).[9] In addition, a double-reciprocal plot of the inverse of the rate of reaction versus the inverse of the O_2 concentration reveals that the linear plots corresponding to the different αKG concentrations intersect on the *y*-axis, suggesting that αKG is a competitive inhibitor with respect to O_2 (Figure 3).[b] Importantly, a competitive inhibition of O_2 by αKG has

dx.doi.org/10.1021/bi3012466 | *Biochemistry* 2012, 51, 8699–8701

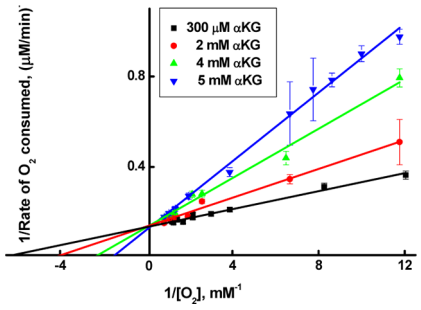

Figure 3. Double-reciprocal plot of 1/rate of O_2 consumed vs $1/[O_2]$ obtained using the O_2 consumption assay, suggesting αKG competitive inhibition of JMJD2C with respect to O_2.

not been observed for any αKG-dependent oxygenase to date.[7i,15] Moreover, the more pronounced αKG inhibition of JMJD2C versus JMJD2A and JMJD2E is expected to impact the different activity profiles in vivo for these enzymes.

The observed αKG substrate inhibition of JMJD2C could have important implications in cancer biology.[8] In normal healthy cells, the expression and activity of JMJD2C are believed to be highly regulated.[6,8] Given the observed in vitro inhibition by αKG, the activity of JMJD2C could be regulated in healthy tissue through a high cellular αKG concentration, which does not allow for an optimal demethylase activity of JMJD2C. Interestingly, there is a large difference in the level of αKG in healthy brain cells and glioblastomas. Whereas in healthy brain tissue the αKG concentration ranges from 1 to 3 mM,[16] it has been reported that the αKG concentration in gliomas and glioblastoma multiformes is 100−300 μM.[17] Indeed, we find that JMJD2C displays its highest activity in vitro at an αKG concentration of ∼300 μM (Figures S3 and S5 of the Supporting Information),[9] suggesting that a decreased concentration of αKG could lead to an increased HDM activity in cancer versus normal cells.[18]

In conclusion, a detailed kinetic analysis of three JmjC-HDMs, including the cancer-relevant JMJD2C, was achieved by employing three enzyme activity assays. Using a continuous O_2 consumption assay, we found that HDMs have affinities for O_2 near the cellular O_2 concentration, suggesting that HDMs may act as oxygen sensors in vivo. Importantly, we have observed a case of αKG substrate inhibition, and the kinetic data suggest that αKG inhibits JMJD2C competitively with respect to O_2. The concentration of αKG at which JMJD2C displays optimal activity in vitro is similar to the concentration of αKG in cancer cells, which has direct implications for the increased activity of JMJD2C in cancer versus normal cells. Future studies will focus on probing the effect of αKG concentration on the activity of HDMs in vivo, as well as the implication of αKG concentration variation in the epigenetic control of cancer versus normal cells.

■ ASSOCIATED CONTENT

Supporting Information

Protein expression and purification, and enzyme kinetic data for FDH, O_2 electrode, and MALDI-TOF MS assays. This material is available free of charge via the Internet at http://pubs.acs.org.

■ AUTHOR INFORMATION

Corresponding Author

*E-mail: mirica@wustl.edu. Phone: (314) 934-3464.

Funding

This work was supported by the Department of Defense through a Breast Cancer Research Program Concept Award (W81XWH-10-1-0442).

Notes

The authors declare no competing financial interest.

■ ADDITIONAL NOTES

[a]The higher K_m (peptide) and lower k_{cat} values obtained through the FDH coupled assay are likely due to the less-than-optimal activity of FDH at high peptide concentrations, (see the Supporting Information).

[b]αKG shows a weak, mixed-mode nonlinear inhibition of JMJD2C with respect to the peptide substrate (Figures S4 and S6 of the Supporting Information).

■ REFERENCES

(1) (a) Klose, R. J., Kallin, E. M., and Zhang, Y. (2006) *Nat. Rev. Genet. 7*, 715−727. (b) Bhaumik, S. R., Smith, E., and Shilatifard, A. (2007) *Nat. Struct. Mol. Biol. 14*, 1008−1016. (c) Mosammaparast, N., and Shi, Y. (2010) *Annu. Rev. Biochem. 79*, 155−179.

(2) (a) Klose, R. J., et al. (2006) *Nature 442*, 312−316. (b) Tsukada, Y., et al. (2006) *Nature 439*, 811−816. (c) Zhang, Y., and Klose, R. J. (2007) *Nat. Rev. Mol. Cell Biol. 8*, 307−318.

(3) (a) Costas, M., Mehn, M. P., Jensen, M. P., and Que, L., Jr. (2004) *Chem. Rev. 104*, 939−986. (c) Loenarz, C., and Schofield, C. J. (2011) *Trends Biochem. Sci. 36*, 7−18.

(4) (a) Chen, Z., et al. (2006) *Cell 125*, 691−702. (b) Ng, S. S., et al. (2007) *Nature 448*, 87−88. (c) Couture, J. F., Collazo, E., Ortiz-Tello, P. A., Brunzelle, J. S., and Trievel, R. C. (2007) *Nat. Struct. Mol. Biol. 14*, 689−695.

(5) (a) Lu, P. J., et al. (1999) *J. Biol. Chem. 274*, 15633−15645. (b) Yamane, K., et al. (2007) *Mol. Cell 25*, 801−812.

(6) Cloos, P. A. C., et al. (2006) *Nature 442*, 307−311.

(7) (a) Rose, N. R., et al. (2008) *J. Med. Chem. 51*, 7053−7056. (b) Rose, N. R., et al. (2010) *J. Med. Chem. 53*, 1810−1818. (c) Hamada, S., et al. (2009) *Bioorg. Med. Chem. Lett. 19*, 2852−2855. (d) Hamada, S., et al. (2010) *J. Med. Chem. 53*, 5629−5638. (e) Chang, K.-H., et al. (2011) *ChemMedChem 6*, 759−764. (f) Lohse, B., et al. (2011) *Angew. Chem., Int. Ed. 123*, 9266−9269. (g) Luo, X., et al. (2011) *J. Am. Chem. Soc. 133*, 9451−9456. (h) Woon, E. C. Y., et al. (2012) *Angew. Chem., Int. Ed. 51*, 1631−1634. (i) Rose, N. R., Mcdonough, M. A., King, O. N. F., Kawamura, A., and Schofield, C. J. (2011) *Chem. Soc. Rev. 40*, 4364−4397.

(8) Liu, G., et al. (2009) *Oncogene 28*, 4491−4500.

(9) See the Supporting Information.

(10) (a) Shi, Y., et al. (2004) *Cell 119*, 941−953. (b) Roy, T. W., and Bhagwat, A. S. (2007) *Nucleic Acids Res. 35*, e147.

(11) Mirica, L. M., and Klinman, J. P. (2008) *Proc. Natl. Acad. Sci. U.S.A. 105*, 1814−1819.

(12) (a) Krishnan, S., Collazo, E., Ortiz-Tello, P. A., and Trievel, R. C. (2012) *Anal. Biochem. 420*, 48−53. (b) Kristensen, L. H., et al. (2012) *FEBS J. 279*, 1905−1914.

(13) Hirsila, M., Koivunen, P., Gunzler, V., Kivirikko, K. I., and Myllyharju, J. (2003) *J. Biol. Chem. 278*, 30772−30780.

(14) (a) Chowdhury, R., et al. (2011) *EMBO Rep. 12*, 463−469. (b) Sakurai, M., et al. (2010) *Mol. BioSyst. 6*, 357−364.

(15) (a) Holme, E. (1975) *Biochemistry 14*, 4999−5003. (b) Dubus, A., et al. (2001) *Cell. Mol. Life Sci. 58*, 835−843. (c) Welford, R. W. D., Schlemminger, I., Mcneill, L. A., Hewitson, K. S., and Schofield, C. J. (2003) *J. Biol. Chem. 278*, 10157−10161.

(16) Thirstrup, K., et al. (2011) *Pharmacol. Res. 64*, 268−273.

(17) (a) Dang, L., et al. (2009) *Nature 462*, 739−744. (b) Gross, S., et al. (2010) *J. Exp. Med. 207*, 339−344.

(18) Xu, W., et al. (2011) *Cancer Cell 19*, 17−30.

Dalton Transactions

Dynamic Article Links
View Online

Cite this: *Dalton Trans.*, 2012, **41**, 8010

www.rsc.org/dalton

PAPER

Cycloaddition reactivity studies of first-row transition metal–azide complexes and alkynes: an inorganic click reaction for metalloenzyme inhibitor synthesis†

Emi Evangelio,[a] Nigam P. Rath[b] and Liviu M. Mirica*[a]

Received 19th January 2012, Accepted 19th March 2012
DOI: 10.1039/c2dt30145h

The studies described herein focus on the 1,3-dipolar cycloaddition reaction between first-row transition metal–azide complexes and alkyne reagents, *i.e.* an inorganic variant of the extensively used "click reaction". The reaction between the azide complexes of biologically-relevant metals (*e.g.*, Fe, Co and Ni) found in metalloenzyme active sites and alkyne reagents has been investigated as a proof-of-principle for a novel method of developing metalloenzyme triazole-based inhibitors. Six Fe, Co and Ni mono-azide complexes employing salen- and cyclam-type ligands have been synthesized and characterized. The scope of the targeted inorganic azide–alkyne click reaction was investigated using the electron-deficient alkyne dimethyl acetylenedicarboxylate. Of the six metal–azide complexes tested, the Co and Ni complexes of the 1,4,8,11-tetrametyl-1,4,8,11-tetraazacyclotetradecane (Me_4cyclam) ligand showed a successful cycloaddition reaction and formation of the corresponding metal–triazolate products, which were crystallographically characterized. Moreover, use of less electron deficient alkynes resulted in a loss of cycloaddition reactivity. Analysis of the structural parameters of the investigated metal–azide complexes suggests that a more symmetric structure and charge distribution within the azide moiety is needed for the formation of a metal–triazolate product. Overall, these results suggest that a successful cycloaddition reaction between a metal–azide complex and an alkyne substrate is dependent both on the ligand and metal oxidation state, that determine the electronic properties of the bound azide, as well as the electron deficient nature of the alkyne employed.

Introduction

The use of fast, irreversible reactions appropriately called "click reactions" is a simple and popular approach to the synthesis of functionalized molecules by joining two fragments together.[1] These click reactions proceed under mild conditions with quantitative yields and high regioselectivity. Examples of such reactions include nucleophilic ring opening (with epoxides and aziridines), non-aldol type carbonyl reactions (formation of hydrazones and heterocycles), or additions to carbon–carbon multiple bonds (*i.e.*, Michael additions or oxidative formation of epoxides).[1] From this last group, the Huisgen 1,3-dipolar cycloadditions are the most commonly used click reactions.[2] These cycloaddition reactions involve a 1,3-dipole (*i.e.*, an azide) and an unsaturated dipolarophile (*e.g.*, an alkyne, Scheme 1, i). Among various types of 1,3-dipoles, organic azides are particularly important as they provide an entry into the synthesis of triazoles and tetrazoles.[2] These heterocycle derivatives have found use in important applications such as pharmaceuticals, chemical biology,[3] or energetic materials.[4]

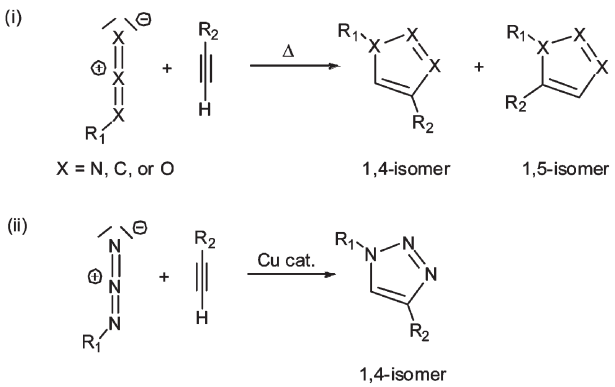

Scheme 1 (i) Huisgen 1,3-dipolar cycloaddition; (ii) Cu-catalyzed azide–alkyne cycloaddition (CuAAC).

Since the first report of a regioselective 1,3-dipolar cycloaddition reaction in 2002,[5] tremendous scientific efforts have been devoted to studying these click reactions. The Cu-catalyzed

[a]*Department of Chemistry, Washington University in St. Louis, One Brookings Drive, St. Louis, Missouri 63130-4899, USA. E-mail: mirica@wustl.edu; Fax: (+1)-314-935-4481*
[b]*Department of Chemistry and Biochemistry and Center for Nanoscience, University of Missouri-St. Louis, One University Boulevard, St. Louis, Missouri 63121-4400, USA*

†CCDC reference numbers 864402–864408. For crystallographic data in CIF or other electronic format see DOI: 10.1039/c2dt30145h

azide–alkyne cycloaddition reaction (CuAAC) (Scheme 1, ii) occurs in various solvents at room temperature and the 1,4-substituted isomer is obtained regioselectively. All these characteristics make the CuAAC an excellent prototype for the click reaction.

The catalyst-free AAC reaction has also led to the development of "*in situ* click reactions" in enzyme inhibitor design for drug discovery,[6] in which the targeted enzymes are allowed to assemble new inhibitors by linking azides and alkynes that bind to adjacent sites on the protein.[7,8] The increase in their local concentration likely accelerates the cycloaddition reaction, a high-affinity inhibitor being formed (Scheme 2a).[7] Thus, the enzyme itself, serving as the reaction vessel, promotes the synthesis of its highest-affinity inhibitor. In contrast, although metal ions are used as catalysts for the cycloaddition reaction,[5] the reaction between a metalloenzyme–azide adduct and an alkyne-derived substrate has not been explored for metalloenzymes (Scheme 2b).[9]

In this context, we are interested in studying the cycloaddition reaction between a metal–azide complex and an alkyne (*i.e.*, an "inorganic" click reaction) as a proof-of-concept for the enzyme-templated reaction.[10] Performing this reaction at the active site of a metalloenzyme and using an alkyne substrate analogue should lead to a novel approach for the synthesis of high-affinity inhibitors. A successful cycloaddition reaction would lead to formation of the triazole product, which can be detected upon protein denaturation. The identified triazoles can then be independently synthesized through a non-enzymatic methodology and used for enzyme inhibition studies.

A survey of the literature reveals that reactions between metal–azide complexes and electron deficient alkynes have been observed for a few neutral Co[11] and Ni[12] coordination compounds, as well as several organometallic complexes of Ta,[13] Ru,[14–16] Fe,[15] Mn,[17] Au,[18] Os,[19] and Mo[20] (Scheme 3). In addition, a "fully" inorganic click reaction between a metal–azide and a metal–acetylide has been reported recently.[21] By contrast, such cycloaddition reactions for biomimetic metal complexes with N- and O-donor ligand systems are much more rare.[11a,12] In this context, several Fe–, Co– and Ni–azide

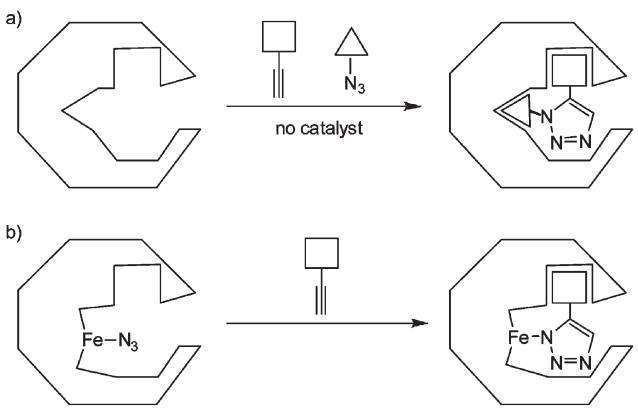

Scheme 2 (a) Use of the azide–alkyne cycloaddition (AAC) reaction to synthesize a high-affinity inhibitor from two inhibitors with different binding sites (ref. 7); (b) an inorganic azide–alkyne cycloaddition reaction proposed herein as a novel metalloenzyme inhibitor design strategy.

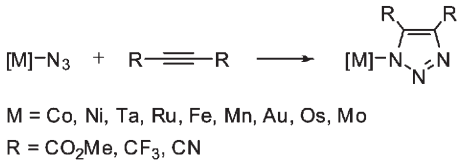

Scheme 3 Reported reactions between metal–azide complexes and electron-deficient alkynes.

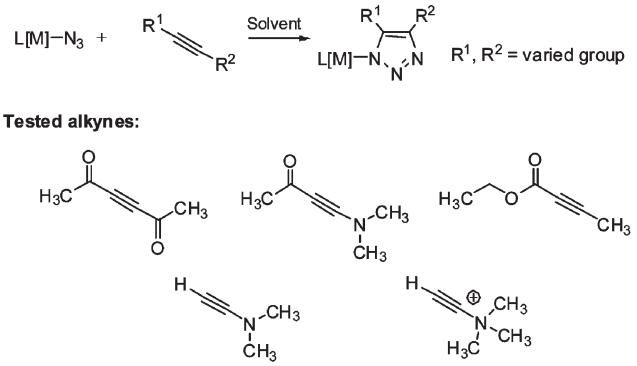

Scheme 4 Targeted synthesis of metal–triazolate complexes through the cycloaddition of metal–azide complexes and alkynes. The ligands employed are shown in Scheme 5.

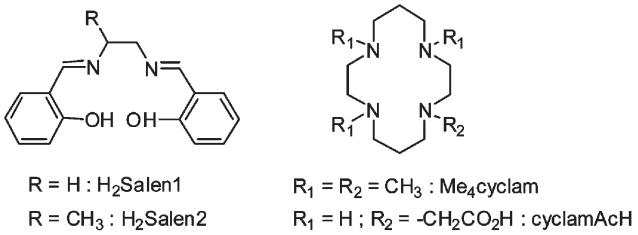

Scheme 5 Biomimetic ligands employed in this study.

complexes that are structural models of metalloenzyme active sites[22] have been synthesized and their cycloaddition reactivity toward alkynes has been investigated (Schemes 4 and 5). The reaction of these azide complexes with different alkynes was studied to determine the scope of the cycloaddition chemistry with respect to the metal coordination geometry and oxidation state, as well as the electronic properties of the alkyne reagent.

Results and discussion

Synthesis of salen-type ligands

The metal–azide complexes employing salen-type ligands have been synthesized following literature procedures and employing two ligands, *N*,*N*′-bis(salicylidene)-1,2-ethylenediimine (H_2salen1) and *N*,*N*′-bis(salicylidene)-1,2-propylenediimine (H_2salen2, Scheme 5). H_2Salen1 and H_2Salen2 were synthesized by condensation of 2 equiv. salicylaldehyde and 1 equiv. ethylenediamine or 1,2-diaminopropane,[23] respectively, in ethanol over a period of 2 h.

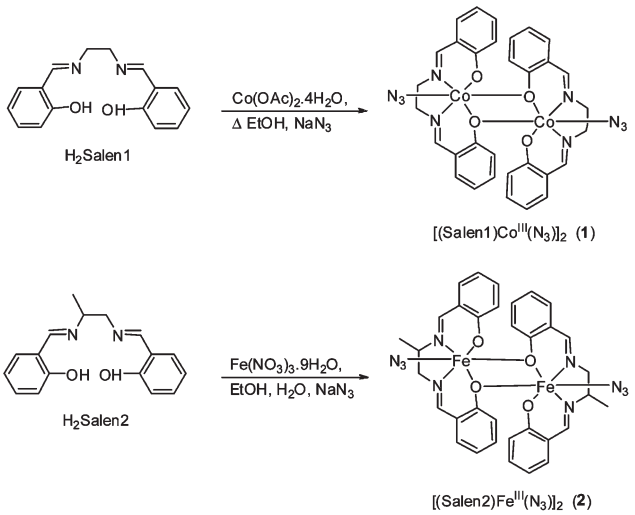

Scheme 6 Synthetic method for the synthesis of metal–azide complexes with H_2Salen1 and H_2Salen2.

A solution of H_2Salen1 was mixed with equimolar solutions of cobalt acetate in ethanol and sodium azide in water (Scheme 6), and slow evaporation of the filtered solution led to crystallization of $[(salen1)Co^{III}(N_3)]_2$, **1** (Table 1). When the same reaction is performed with H_2Salen2 and iron nitrate (Scheme 6), crystals of $[(salen2)Fe^{III}(N_3)]_2$, **2** were obtained. Similarly, the $[(salen1)Fe^{III}(N_3)]_2$ and $[(salen2)Co^{III}(N_3)]_2$ complexes were synthesized and characterized by ESI-MS, however no pure crystalline products could be obtained. Interestingly, formation of a mononuclear $[(salen2)Fe^{III}N_3]$ complex was reported previously under similar reaction conditions,[23a] although the room-temperature X-ray structure for that complex reveals intermolecular Fe–O interactions analogous to those observed for **2**.

Structures of $[(salen1)Co^{III}(N_3)]_2$ (1) and $[(salen2)Fe^{III}(N_3)]_2$ (2)

The asymmetric unit of both **1** and **2** consists of one-half of the dinuclear structure, the other half being generated by projection through a crystallographic inversion centre. Fig. 1 shows the molecular structure and atom labelling of both complexes. The two M^{III} ions of the two dinuclear complexes are bridged by two phenolate μ-O atoms. The octahedral coordination of each M^{III} ion is completed by the tetradentate Schiff-base ligand and a terminal N_3^- ion. The two N_3^- ligands are *trans* relative to the M–M vector, as imposed by the crystallographic inversion centre.

The M1–O2^i bond is longer than the M1–O2 bond (Table 2) is likely due to either the greater *trans* influence of the N_3^- compared to the imine N atom[23b] or a better orbital overlap of the O2 atom with the metal centre. The M1–N3 distances (1.932 Å for cobalt and 2.015 Å for iron complexes, respectively) are in the range of the other M^{III} complexes reported in the literature.[23a,24] The M1–O2 bond is longer than the M1–O1 bond due to the interaction of O2 with M1^i. The average M–N(imine) bond length is 1.883 and 2.103 Å for cobalt and iron complexes, respectively. The three *trans* angles at the M^{III} atom are between 158.6 and 177.6°. The distorted octahedral geometry of the

Table 1 Crystallographic data for $[(salen1)Co^{III}(N_3)]_2$ (**1**), $[(salen2)Fe^{III}(N_3)]_2$ (**2**), $[(Me_4cyclam)Ni^{II}(N_3)]PF_6$ (**3**), $[(Me_4cyclam)Co^{II}(N_3)]ClO_4$ (**4**), $[(cyclamAc)Co^{III}(N_3)]ClO_4$ (**6**), $\{(Me_4cyclam)\text{-}Ni^{II}[N_3C_2(CO_2Me)_2]\}ClO_4$ (**7**) and $[\{(Me_4cyclam)Co^{II}[N_3C_2(CO_2Me)_2]\}ClO_4$ (**8**)

	1	2	3	4	6	7	8
Formula	$C_{34}H_{32}Cl_4Co_2N_{10}O_4$	$C_{34}H_{32}Fe_2N_{10}O_4$	$C_{14}H_{32}F_6N_7NiP$	$C_{14}H_{32}ClCoN_7O_4$	$C_{12}H_{25}ClCoN_7O_6$	$C_{20}H_{38}ClN_7NiO_8$	$C_{20}H_{38}ClCoN_7O_8$
M_r	904.36	756.40	502.15	456.85	457.77	598.73	598.95
Color	Brown plates	Red plates	Green needles	Violet plates	Violet plates	Blue plates	Red plates
Crystal system	Monoclinic	Monoclinic	Orthorhombic	Orthorhombic	Orthorhombic	Monoclinic	Monoclinic
Space group	$P2_1/n$	$P2_1/n$	*Pnma*	$Pna2_1$	*Pbca*	*C2/c*	*C2/c*
a/Å	9.1697(7)	8.5467(9)	14.4194(15)	13.9561(9)	13.4690(11)	12.2771(7)	12.4963
b/Å	14.4120(10)	13.5994(16)	9.7386(10)	15.2417(10)	13.3584(12)	15.7842(9)	16.1164(15
c/Å	13.6075(11)	14.4097(18)	14.4293(15)	9.2732(5)	20.0722(14)	14.1558(8)	14.2264(14)
β/°	91.467(3)	103.693(6)	90	90	90	104.624(3)	105.206(5)
V/Å^3	1797.7(2)	1627.2(3)	2026.2(4)	1972.5(2)	3611.5(5)	2654.3(3)	2764.8(5)
Z	2	2	4	4	8	4	4
T/K	100(2)	100(2)	100(2)	100(2)	100(2)	100(2)	293(2)
λ/Å	0.71073	0.71073	0.71073	0.71073	0.71073	0.71073	0.71073
D_c/g cm^{-3}	1.671	1.544	1.646	1.538	1.684	1.498	1.439
μ/mm^{-1}	1.276	1.544	1.107	1.042	1.146	0.889	0.772
R, R_w[a]	0.0322, 0.0702	0.1011, 0.1458	0.0361, 0.0740	0.0244, 0.0506	0.0734, 0.0853	0.0512, 0.1094	0.0591, 0.1599

[a] $R = \sum||F_o| - |F_c||/\sum|F_o|$; $R_w = [\sum w(|F_o| - |F_c|^2/\sum w(F_o)^2]^{1/2}$.

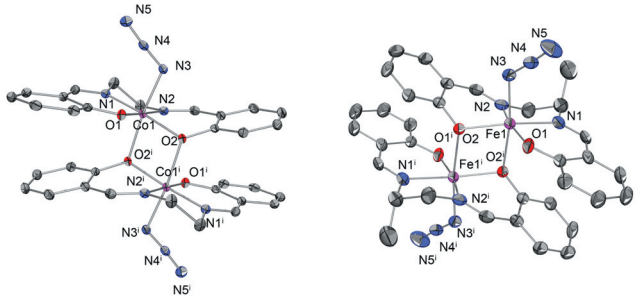

Fig. 1 View of the molecular structure and atom labelling of (left) $[(salen1)Co^{III}(N_3)]_2$ (**1**) and (right) $[(salen2)Fe^{III}(N_3)]_2$ (**2**). Hydrogen atoms have been omitted for clarity.

metal centre is also suggested by the *cis* angles that vary from 77.7 to 107.5° in the case of the Fe complex, and from 85.5° to 95.0° for the Co complex. As a result of the centre of symmetry, the M_2O_2 core of both complexes is perfectly planar.

Synthesis of cyclam-type ligands

The cyclam-type ligands were chosen based on their ability to stabilize mononuclear metal–azide complexes that are more structurally similar to the metalloenzyme active sites. As such, 1,4,8,11-tetrametyl-1,4,8,11-tetraazacyclotetradecane (Me_4cyclam) and 1,4,8,11-tetraazacyclotetradecane-1-acetic acid (cyclamAcH) were chosen for the synthesis of metal–azide complexes (Scheme 5). The synthesis of Me_4cyclam (Scheme 7) has been successfully accomplished following a literature procedure[25] to obtain the ligand in high yield. The isolated product is highly hygroscopic and was dried under vacuum for 2 h at 50 °C before the metal complexation reaction. The synthesis of the cyclamAcH ligand was also accomplished by employing a modified version of a published procedure (Scheme 7),[26] a higher yield of the product being obtained by extending the reaction time to 4 h, washing with $CHCl_3$, and treating the final product with HCl (*vide infra*).

Synthesis and structures of metal–azide complexes derived from cyclam-type ligands

As described in the literature,[27] mononuclear metal–azide complexes derived from the Me_4cyclam ligand were obtained for Co and Ni: $[(Me_4cyclam)Ni^{II}(N_3)]^+$ (**3**) and $[(Me_4cyclam)Co^{II}(N_3)]^+$ (**4**), respectively. Mixing of 1 equiv. ligand with 1 equiv. Ni or Co perchlorate in ethanol, followed by addition of 5 equiv. aqueous NaN_3 and heating at 70 °C for 1 h led to formation of green or violet crystals upon standing at low temperature. A summary of the X-ray experimental data is provided in Table 1.

The crystal structure of these compounds (Fig. 2) and the bond lengths and angles (Table 2) are similar to those previously reported.[27] The cyclam adopts the *trans*-I configuration as described by Bosnich *et al.*,[28] which is the most favoured configuration for this kind of complexes. The four methyl substituents of the ring are positioned on the same side of the molecule as the azide ligand, which fits into the cavity formed by the methyl groups. The coordination geometry of the metal centre varies from square pyramidal for the nickel complex (τ value of ~0) to a more distorted trigonal bipyramidal geometry for the cobalt complex (τ value of 0.45).[29]

For first-row transition metals, the coordination chemistry of monofunctionalized cyclam derivatives has mainly focused on complexes of Ni^{II}, Cu^{II} and Co^{II}.[30] In 2000, Wieghardt *et al.*, described the synthesis and characterization of a monofunctionalized Fe^{III} complex of 1,4,8,11-tetraazacyclotetradecane-1-acetic acid, cyclamAcH, as a precursor for the synthesis of high-valent Fe complexes.[22] As described therein, the cyclamAcH ligand provides upon deprotonation a monoanionic pentacoordinate framework for the synthesis of a series of complexes with a single, variable coordination site. Thus, the cyclamAcH ligand is particularly appealing for our studies. In addition, the presence of a carboxylate group makes the corresponding metal complexes more similar to the coordination environment found in non-heme iron enzymes, where a carboxylate group coordinates to the Fe centre.[31] The synthesis of the cyclamAcH complexes was performed as described by Wieghardt *et al.* with a slight variation (Scheme 8). Ferric chloride was treated with cyclamAcH in a refluxing aqueous solution for 90 min. After cooling this solution at room temperature and addition of an excess of sodium azide, a clear red solution formed after 2 h. Addition of an excess of KPF_6 yields a microcrystalline solid of $[(cyclamAc)Fe^{III}(N_3)]PF_6$ (**5**) upon cooling at 4 °C overnight. This compound was fully characterized by ESI-MS, UV-vis and IR spectroscopy, and the results are in full agreement with the compound previously described.[22]

When the same reaction is performed in the presence of $Co(ClO_4)\cdot 6H_2O$, a dark violet powder is obtained. Crystals of $[(cyclamAc)Co^{III}(N_3)]ClO_4$ (**6**) were obtained by slow diffusion of diethyl ether in an acetonitrile solution. A summary of the X-ray experimental data is provided in Table 1. A representation of the $[(cyclamAc)Co^{III}(N_3)]^+$ cation is shown in Fig. 3, with selected bond distances and angles listed in Table 2.

The Co^{III} ion sits in a compressed octahedral environment with three of the four ligand N atoms (*i.e.*, N1, N4 and N3) occupying the equatorial positions along with the carboxylate O atom (Fig. 3); the fourth N atom (N2) occupies one of the axial sites with the azide ligand situated *trans* to the N2 atom. By contrast to the *trans*-III ligand configuration in **5**,[22] the cyclamAc ligand adopts the *cis*-V[28] configuration in **6**, which implies a dramatic configuration change. The complex exhibits a longer Co–N2 distance (1.994 Å) compared to the Co–N1 (1.962 Å) and Co–N3 (1.982 Å) distances, as expected for the slightly stronger *trans* influence of the carboxylate group. The Co–N3 bond distance (1.982 Å) is slightly longer than the Co–N1 distance (1.962 Å), likely due to the presence of the acetate arm bonded to N3. The $Co–N_{azide}$ and $Co–O_{acetate}$ distances are 1.936 and 1.899 Å, similar to those reported for the iron complex.[21] To the best of our knowledge, complex **6** represents the first example of a cyclamAc metal complex where the macrocyclic ligand adopts the less-common *cis*-V configuration.[32]

IR characterization of the metal–azide complexes

For all metal–azide complexes synthesized, their characteristic azide stretches were measured by IR spectroscopy. Spectra were

Table 2 Selected bond distances (Å) and angles (°) for [(salen1)$Co^{III}(N_3)]_2$ (**1**), [(salen2)$Fe^{III}(N_3)]_2$ (**2**), [$(Me_4cyclam)Ni^{II}(N_3)]PF_6$ (**3**), [$(Me_4cyclam)Co^{II}(N_3)]ClO_4$ (**4**), [$(cyclamAc)Co^{III}(N_3)]ClO_4$ (**6**), {$(Me_4cyclam)Ni^{II}[N_3C_2(CO_2Me)_2]\}ClO_4$ (**7**) and [{$(Me_4cyclam)$-$Co^{II}[N_3C_2(CO_2Me)_2]\}ClO_4$ (**8**)

	1	2		3	4		6		7	8
M1–N1	1.8738(13)	2.087(4)	M1–N1	2.1959(8)	2.1192(15)	Co–N1	1.962(2)	M1–N1	2.1131(12)	2.1990(19)
M1–N2	1.8916(14)	2.118(4)	$M1–N1^i$	2.1295(8)	2.1136(15)	Co–N2	1.994(2)	$M1–N1^i$	2.1131(12)	2.1990(19)
M1–N3	1.9319(14)	2.015(4)	M1–N2	2.1323(8)	2.2184(15)	Co–N3	1.982(2)	M1–N2	2.1472(13)	2.1292(18)
M1–O1	1.8798(11)	1.881(3)	$M1–N2^i$	2.1323(8)	2.2357(15)	Co–N4	1.972(2)	$M1–N2^i$	2.1472(13)	2.1292(18)
M1–O2	1.9333(11)	1.981(3)	M1–N3	1.9887(12)	1.9742(13)	Co–N5	1.936(2)	M1–N3	2.0017(17)	2.030(3)
$M1–O2^i$	2.0217(11)	2.169(3)	N3–N4	1.1805(18)	1.183(2)	Co–O1	1.8995(11)	N3–N4	1.3304(15)	1.326(2)
$O2–M1^i$	2.0216(11)	2.169(3)	N5–N5	1.153(2)	1.160(2)	C12–O1	1.283 (3)	$N3–N4^i$	1.3304(15)	1.326(2)
N3–N4	1.209(2)	1.209(5)				C12–O2	1.224(3)			
N4–N5	1.150(2)	1.132(6)				N5–N6	1.208(3)			
						N6–N7	1.151(3)			
O2–M1–O1	88.01(5)	107.51(13)	$N1–M1–N1^i$	94.24(5)	93.34(6)	N4–Co–N1	85.79(9)	$N1–M1–N1^i$	147.39(8)	167.65(12)
O2–M1–N2	91.64(5)	84.40(14)	$N2–M1–N2^i$	91.68(5)	92.11(6)	N4–Co–N3	94.33(9)	$N2–M1–N2^i$	171.73(8)	140.94(12)
O1–M1–N2	177.65(5)	165.83(14)	N1–M1–N2	84.86(3)	83.27(6)	N3–Co–O1	87.29(8)	N1–M1–N2	85.13(5)	83.91(8)
O2–M1–N1	174.22(5)	158.61(15)	$N1^i–M1–N2^i$	84.85(3)	83.78(6)	N1–Co–O1	92.61(9)	$N1^i–M1–N2^i$	85.13(5)	83.91(8)
O1–M1–N1	95.04(5)	88.56(15)	$N2^i–M1–N1$	164.09(3)	141.50(6)	N1–Co–N3	179.42(9)	$N2^i–M1–N1$	92.54(5)	91.96(8)
N2–M1–N1	85.51(6)	78.08(16)	$N2–M1–N1^i$	164.09(3)	168.63(5)	N4–Co–O1	177.21(8)	$N2–M1–N1^i$	92.54(5)	91.96(8)
$O2–M1–O2^i$	81.46(5)	77.75(12)	N2–M1–N3	94.32(4)	94.18(6)	N2–Co–N5	175.68(10)	N2–M1–N3	94.14(4)	109.53(6)
$O1–M1–O2^i$	93.08(5)	91.48(13)	$N2^i–M1–N3$	94.32(4)	97.19(6)	Co–N5–N6	119.03(18)	$N2^i–M1–N3$	94.14(4)	109.53(6)
$N2–M1–O2^i$	89.17(5)	83.43(13)	N1–M1–N3	101.42(3)	109.03(7)	N5–N6–N7	175.4(3)	N1–M1–N3	106.31(4)	96.17(6)
$N1–M1–O2^i$	93.46(5)	88.05(13)	$N1^i–M1–N3$	101.42(3)	109.42(7)			$N1^i–M1–N3$	106.31(4)	96.17(6)
O2–M1–N3	92.32(5)	94.36(14)	M1–N3–N4	133.24(12)	134.22(12)					
O1–M1–N3	89.49(6)	95.53(15)	N3–N4–N5	177.4(2)	178.13(19)					
N2–M1–N3	88.20(6)	91.09(15)								
N1–M1–N3	92.62(6)	98.12(15)								
$O1^i–M1–N3$	173.15(5)	170.76(14)								
M1–N3–N4	117.20(11)	124.6(3)								
N3–N4–N5	175.73(17)	176.4(5)								

measured as thin films obtained from dichloromethane solutions on a NaCl plate. The azide stretching frequencies, $\nu(N_3)_{asym}$, for all these complexes were found between 2015 and 2070 cm^{-1}, typical for such azide adducts (Table 3).

Reaction of metal–azide complexes with dimethyl acetylenedicarboxylate

A summary of the cycloaddition reactions between the synthesized metal–azide complexes and dimethyl acetylenedicarboxylate is shown in Scheme 9. Typically, 1 equiv. of metal–azide complex was treated with an excess of dimethyl acetylenedicarboxylate (4–5 equiv.) in chloroform at room temperature or acetonitrile at 50 °C, and the reaction was followed by IR spectroscopy. The acetonitrile reaction at 50 °C was performed for the complexes where no reaction was observed in chloroform at RT. In the cases when the 1,3-dipolar cycloaddition occurs, the formation of the N(2)-bound 4,5-bis(methoxycarbonyl)-1,2,3-triazolate complex was confirmed by the disappearance of the $\nu(N_3)_{asym}$ stretch in the IR spectrum and the appearance of sharp peaks assigned to the stretching frequencies of the C═O, N═N and C–O bonds, and ring vibrations of the triazolate product, as reported previously.[11a,19]

When the cycloaddition reaction was attempted for the (salen)Co– and (salen)Fe–azide complexes **1** and **2**, no decrease in the intensity of the azide stretching frequency was observed even after 6 days, either at RT or 50 °C in chloroform or acetonitrile, indicating that the cycloaddition reaction does not occur for these complexes. For both **1** and **2**, the potential dissociation of the dinuclear complexes into mononuclear species in solution needs to be considered; however, the weak axial metal–O interactions (*vide supra*) are not expected to have an appreciable effect on the rate of the azide–alkyne cycloaddition reaction for the dinuclear *vs.* mononuclear species.

Interestingly, treatment of 1 equiv. of [$(Me_4cyclam)Ni^{II}(N_3)$]-PF_6 (**3**) with 5 equiv. of dimethyl acetylenedicarboxylate under stirring in $CHCl_3$ at RT shows the complete disappearance of the azide peak (2070 cm^{-1}) after 6 h and the appearance of stretches at 1726 cm^{-1} (ν(C═O)), 1480 cm^{-1} (ν(N═N)),[19] 1270 cm^{-1} (ν(C–O)), and triazolate ring vibrations at 826, 806 and 778 cm^{-1}, corresponding to the formation of a triazolate species (Fig. 4).[11] Crystals of the product {$(Me_4cyclam)Ni^{II}[N_3C_2$-$(CO_2Me)_2]\}$ ClO_4 (**7**) were obtained by slow diffusion of hexane into a dichloromethane solution. Similar results were obtained for [$(Me_4cyclam)Co^{II}(N_3)]ClO_4$ (**4**), which was treated with 5 equiv. dimethyl acetylenenedicarboxylate in chloroform to lead to the disappearance of the azide stretch at 2070 cm^{-1} and appearance of stretches at 1728, 1479, 1261 cm^{-1}, and triazolate ring vibrations at 822, 805 and 779 cm^{-1}, respectively.[11a,19] Crystals of {$(Me_4cyclam)Co^{II}[N_3C_2(CO_2Me)_2]\}ClO_4$ (**8**) were obtained by slow diffusion of hexane into a dichloromethane solution of the isolated product.

By contrast, when the (cyclamAc)Fe– and (cyclamAc)Co–azide complexes **5** and **6** were treated with an excess of dimethyl acetylenedicarboxylate, no disappearance of the azide stretch at 2052 cm^{-1} was observed even after 5 days, either in acetonitrile or chloroform at RT or 50 °C. Overall, the lack of a cycloaddition reaction suggests that subtle changes in the electronic properties and ligand environment of the metal centre

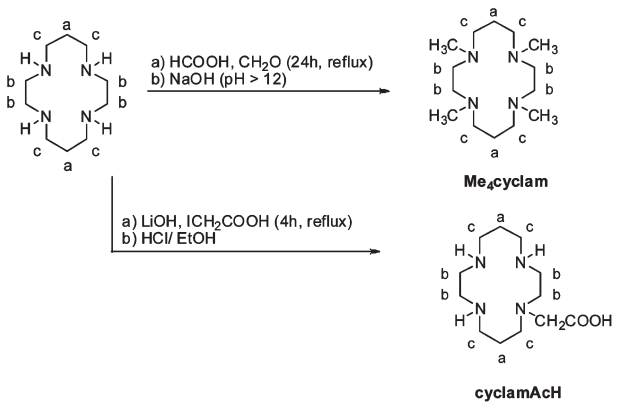

Scheme 7 Synthesis of cyclam-derived ligands.

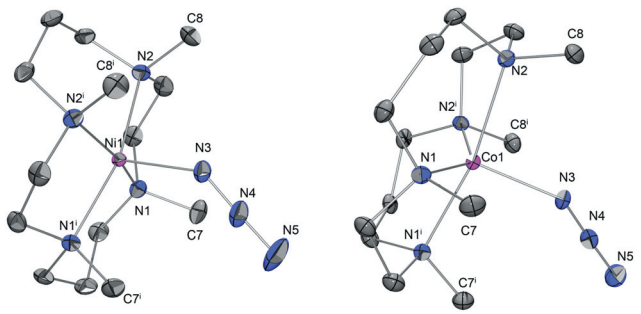

Fig. 2 View of the molecular structure and atom labelling of the mono-cations of (left) $[(Me_4cyclam)Ni^{II}(N_3)]PF_6$ (**3**) and (right) $[(Me_4cyclam)Co^{II}(N_3)]ClO_4$ (**4**). The counteranions and hydrogen atoms have been omitted for clarity.

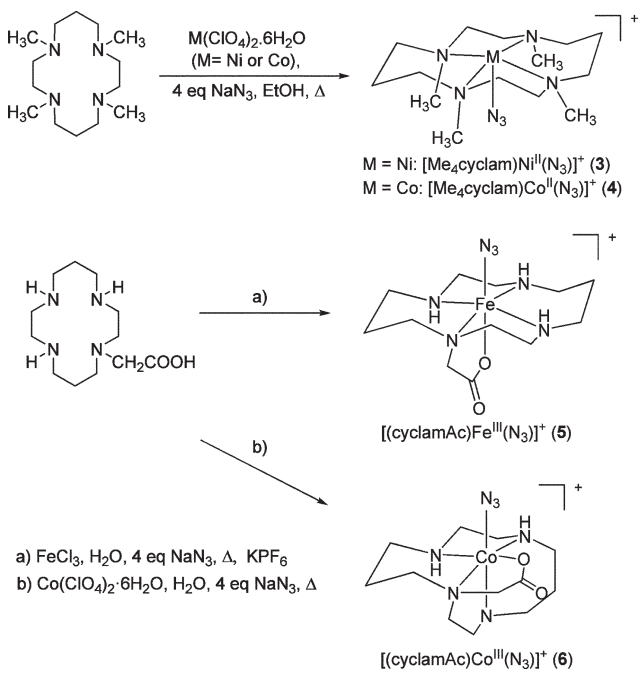

Scheme 8 Synthesis of metal–azide complexes using cyclam-derived ligands.

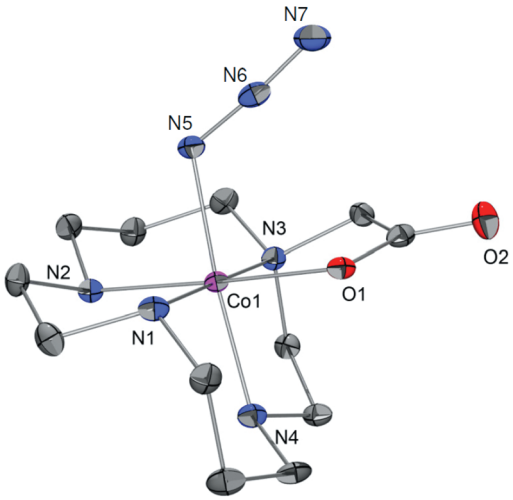

Fig. 3 View of the molecular structure and atom labelling of the mono-cation of $[(cyclamAc)Co^{III}N_3]ClO_4$ (**6**). The counter-anion and hydrogen atoms have been omitted for clarity.

Table 3 Azide stretching frequencies, $\nu(N_3)_{asym}$, for the metal–azide complexes described herein. IR spectra were measured as thin films

Complex	$\nu(N_3)_{asym}/cm^{-1}$
$[(salen1)Co^{III}(N_3)]_2$	2015
$[(salen2)Fe^{III}(N_3)]_2$	2058
$[(Me_4cyclam)Ni^{II}N_3]PF_6$[a]	2070
$[(Me_4cyclam)Co^{II}N_3]ClO_4$	2070
$[(cyclamAc)Fe^{III}N_3]PF_6$[b]	2046
$[(cyclamAc)Co^{III}N_3]ClO_4$	2052

[a] Lit. value 2066 cm^{-1} (ref. 27*b*). [b] Lit. value 2051 cm^{-1} (ref. 22).

are critical in the successful formation of the triazolate product (*vide infra*).

Structures of metal–triazolate complexes 7 and 8

Complexes $\{(Me_4cyclam)Co^{II}[N_3C_2(CO_2Me)_2]\}ClO_4$ (**7**) and $\{(Me_4cyclam)Ni^{II}[N_3C_2(CO_2Me)_2]\}ClO_4$ (**8**) were characterized by X-ray single crystal analysis (Fig. 5). The experimental crystallographic data are summarized in Table 1 and selected bond lengths and angles are given in Table 2.

Both complexes **7** and **8** crystallize in the same space group (monoclinic *C*2/*c*). In both structures the metal ion exhibits a square-pyramidal coordination geometry where the N atoms of the Me_4cyclam ligand occupy the equatorial positions and the triazolate anion is bound axially (Fig. 5). The 4,5-bis(methoxy-carbonyl)-1,2,3-triazolate ligand binds symmetrically to the metal centre, through its central N(3) atom, and the triazole plane adopts a staggered orientation relative to the methyl groups of Me_4cyclam in order to minimize steric repulsions. Given this C_2 symmetry of the cations of **7** and **8**, the two sets of equivalent $M–N_{ligand}$ distances are 2.113 and 2.147 Å for the Ni complex and 2.129 and 2.199 Å for the Co complex, while the $M–N_{triazole}$ distances are 2.002 and 2.030 Å for **7** and **8**, respectively (Table 2). To the best of our knowledge, complexes **7** and **8**

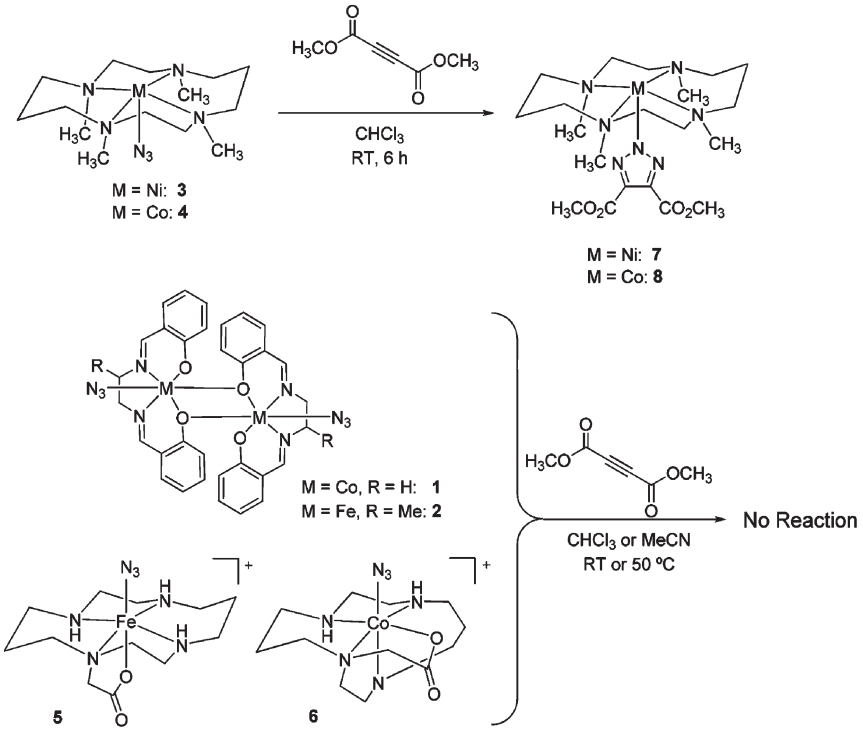

Scheme 9 Survey of the cycloaddition reaction for various metal–azide complexes and the electron-deficient alkyne dimethyl acetylenedicarboxylate.

represent the first structurally characterized Ni^{II}– and Co^{II}–triazolate complexes formed upon a cycloaddition reaction; only one other structurally characterized Co^{III}–triazolate complex has been reported to date.[33] Moreover, **7** and **8** are the first metal–triazolate complexes with a five-coordinated geometry around the metal ion.[32]

Factors determining the cycloaddition reaction for metal–azide complexes

In order to discern the factors that lead to a successful cycloaddition reaction between an alkyne and various metal–azide complexes, we compared relevant metrical parameters of the azide complexes obtained herein and two other structurally characterized Co^{III}–azide complexes[33,34] that have been previously shown to undergo a cycloaddition reaction with dimethyl acetylenedicarboxylate.[11] Analysis of metrical parameters reveals that metal–azide complexes that lead to triazole formation exhibit longer metal–azide bonds (>1.955 Å, Table 4), which could be due to either the presence of axial donors with stronger *trans* influence (*e.g.*, PPh_3 or py),[11] or the presence of metal centers in lower oxidation states (*e.g.*, Ni^{II} and Co^{II}). However, while the Fe–azide bond length in $[(salen2)Fe^{III}(N_3)]_2$ is 2.015 Å, no cycloaddition reaction was observed for this complex. By contrast, shorter proximal N–N bonds ($N–N_{prox}$) of the bound azide ligand are observed for the complexes undergoing the cycloaddition reaction (Table 4). In addition, the difference between the long and short N–N bonds of the azide ligand (*i.e.*, $N–N_{prox}$ and $N–N_{dist}$, respectively) is smaller (<0.029 Å) for these complexes *vs.* those that do not form

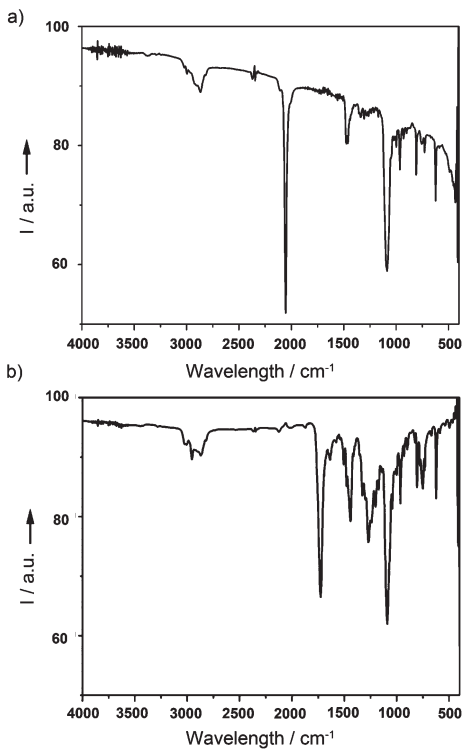

Fig. 4 The cycloaddition reaction between $[(Me_4cyclam)Ni^{II}(N_3)]ClO_4$ and dimethyl acetylenedicarboxylate in $CHCl_3$ monitored by IR: (a) before addition of alkyne and (b) after 6 h.

triazolate adducts (>0.053 Å). This bond length difference ($N–N_{prox} - N–N_{dist}$) provides a measure of the contribution of

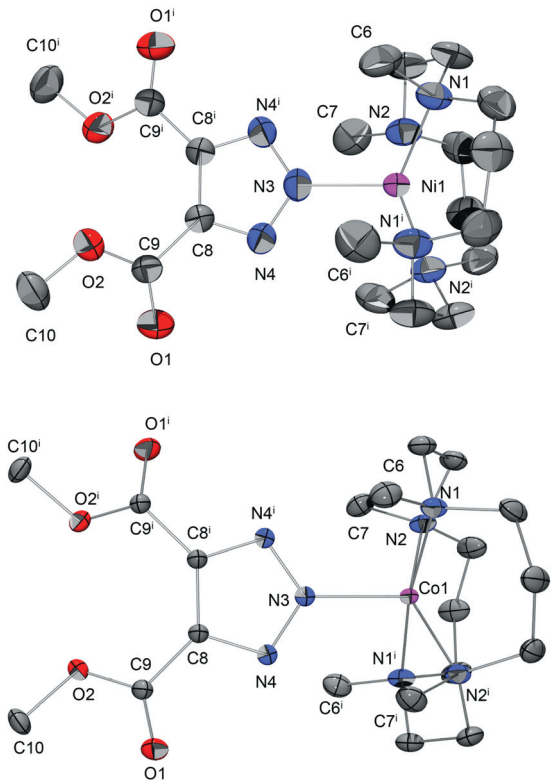

Fig. 5 View of the molecular structure and atom labelling of the mono-cation of (top) {(Me$_4$cyclamNi^{II}[N$_3$C$_2$(CO$_2$Me)$_2$]}ClO$_4$ (**7**) and (bottom) {(Me$_4$cyclamCo^{II}[N$_3$C$_2$(CO$_2$Me)$_2$]}ClO$_4$ (**8**). The counteranion and hydrogen atoms have been omitted for clarity.

the two possible resonance forms (*a*) or (*b*) to the electronic structure of the metal–azide complexes, and strongly suggests that the azide groups with a greater contribution from the resonance form (*b*) (*i.e.*, with a more symmetric charge density distribution) are expected to undergo the cycloaddition reaction more easily.

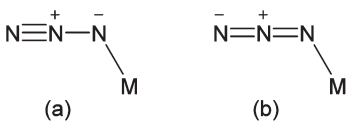

Reaction of metal–azide complexes with other alkynes

Our results suggest that the Ni– and Co–azide complexes **7** and **8** with the Me$_4$cyclam ligand can undergo a cycloaddition reaction with dimethyl acetylenedicarboxylate to yield the corresponding 1,4-triazolate products. Since the alkyne employed above is very electron deficient, we set out to investigate the click reaction of **7** and **8** with less electron deficient alkynes (Scheme 10). The selected alkynes were chosen as they resemble the methylated amine substrates of the histone demethylase enzymes, a new class of non-heme iron enzymes.[35] The cycloaddition studies were performed similarly to those with dimethyl acetylenedicarboxylate, by adding 5 equiv. alkyne to 1 equiv. metal–azide complex in either chloroform or acetonitrile at RT or 50 °C and followed by IR for the disappearance of the azide

Table 4 Comparison of relevant structural parameters for metal–azide complexes

	d/Å			
Complex	M–N$_3$	N–N$_{prox}$	N–N$_{dist}$	(N–N)$_{prox}$ – (N–N)$_{dist}$
[(salen1)Co^{III}(N$_3$)]$_2$[a]	1.932	1.209	1.150	0.059
[(salen2)Fe^{III}(N$_3$)]$_2$[a]	2.015	1.209	1.132	0.077
[(Me$_4$cyclam)Ni^{II}N$_3$]PF$_6$[a]	**1.989**	**1.180**	**1.153**	**0.027**
[(Me$_4$cyclam)Co^{II}N$_3$]ClO$_4$[a]	**1.974**	**1.183**	**1.160**	**0.023**
[(cyclamAc)Fe^{III}N$_3$]PF$_6$[a]	1.931	1.209	1.156	0.053
[(cyclamAc)Co^{III}N$_3$]ClO$_4$[a]	1.936	1.208	1.151	0.057
(PPh$_3$)Co^{III}(DH)$_2$N$_3$[b]	**2.014**	**1.180**	**1.161**	**0.019**
(py)Co^{III}(DH)$_2$N$_3$[c]	**1.955**	**1.155**	**1.126**	**0.029**

The azide adducts highlighted in bold yield triazole products.[a] This work. [b] Ref. 33. [c] Ref. 34, DH = dimethylglyoximato.

stretch and the appearance of the triazolate product stretches. For all substrates investigated, no triazolate product was obtained when either **7** or **8** was used as the starting material, suggesting that a highly electron deficient alkyne is required for the cycloaddition reaction to occur. Overall, these studies imply that the targeted inorganic azide–alkyne cycloaddition reaction can only occur for a limited set of metal–azide complexes and only when very electron deficient alkynes are employed. Alternatively, use of metal complexes in other oxidation states or stabilized by ligands with various electronic properties may allow for the cycloaddition reaction to proceed for less electron-deficient alkynes. Such additional studies are currently underway.

Conclusion

In summary, we have synthesized and structurally characterized a series of Fe, Co and Ni mono-azide complexes that employ biomimetic salen- and cyclam-derived ligands. The obtained metal–azide complexes were investigated for their ability to undergo an azide–alkyne cycloaddition reaction – an "inorganic click reaction", with several alkyne substates. Our studies reveal that one Co–azide and one Ni–azide complex of the neutral ligand Me$_4$cyclam react with the electron deficient alkyne dimethyl acetylenedicarboxylate to generate the metal–triazolate products, which were structurally characterized. Use of less electron deficient alkynes did not generate the corresponding cycloaddition products. In addition, use of the anionic ligand cyclamAc seems to abolish the ability of the corresponding metal–azide complexes to react with any alkyne, suggesting that even subtle changes in the electronic properties of the metal centre leads to an azide ligand whose polarity renders it unreactive toward a cycloaddition reaction. Analysis of the structural parameters of the investigated metal–azide complexes suggests that a more symmetric charge density distribution within the azide moiety is needed for the formation of the metal–triazolate product. In this context, it will be interesting to study whether the azide adducts of non-heme iron enzymes, as opposed to small inorganic model complexes, are capable of undergoing a cycloaddition reaction with alkyne substrate analogues. It is expected that the active site of these enzymes will promote the "click reaction" to a greater extent than a model complex by

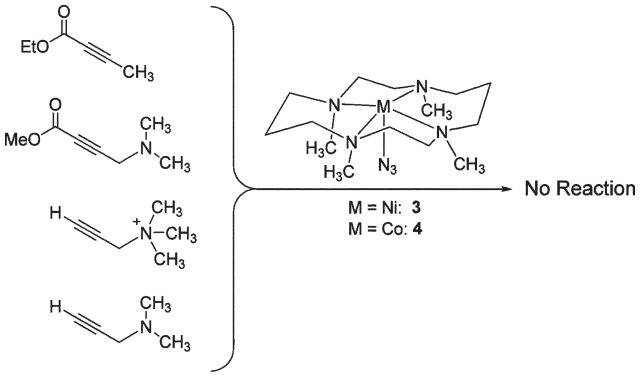

Scheme 10 Alkyne substrates employed in the cycloaddition reaction with the $[(Me_4cyclam)M^{II}(N_3)]ClO_4$ complexes (M = Ni, Co).

increasing the local concentration of the two substrates and thus the rate of the cycloaddition reaction. Our current research efforts are aimed at employing such enzyme-templated cycloaddition reactions for the development of specific inhibitors for non-heme iron enzymes. Of particular interest are histone demethylases, a new class of non-heme iron enzymes that have recently been shown to be overexpressed in cancer cells.[36] Thus, high-affinity histone demethylase inhibitors that exhibit increased specificity can be used in the development of alternative cancer therapeutics.[35]

Experimental section

Commercially available reagents were used as received. All reagents, organic and inorganic, were of high purity grade and obtained from E. Merck, Fluka, Chemie and Aldrich Co. The solvents were dried by passing over an alumina column.

Physical measurements

^{1}H (300.121 MHz) NMR spectra were recorded on a Varian Mercury-300 spectrometer. Chemical shifts are reported in ppm and referenced to residual solvent resonance peaks. Infrared spectra were measured as thin films on a KBr or NaCl plate using a Perkin Elmer Spectrum BX FT-IR spectrometer in the 4000–400 cm^{-1} range. UV-Vis spectra were recorded on a Varian Cary 50 Bio spectrophotometer. ESI-MS experiments were performed on a Bruker Maxis QTOF mass spectrometer with an electron spray ionization source at the Washington University Mass Spectrometry Resource, a NIH Research Resource supported by Grant No. P41RR0954.

X-Ray crystallography

X-Ray diffraction quality crystals of **1**–**4** were obtained by slow evaporation of the mother liqueur. The Co complex **6** was crystallized by slow diffusion of anhydrous diethyl ether into a solution of acetonitrile. The metal–triazolate complexes **7** and **8** were obtained by slow diffusion of hexane in a dichloromethane solution. Suitable crystals of appropriate dimensions were mounted on Mitgen loops in random orientations. Preliminary examination and data collection were performed using a Bruker Kappa Apex-II Charge Coupled Device (CCD) Detector system single-crystal X-Ray diffractometer equipped with an Oxford Cryostream LT device. Data were collected using graphite-monochromated Mo-Kα radiation (λ = 0.71073 Å) from a fine-focus sealed-tube X-ray source. Preliminary unit cell constants were determined with a set of 36 narrow frame scans. Typical data sets consist of a combination of ϖ and ϕ scan frames with typical scan width of 0.5° and counting time of 15–30 s per frame at a crystal to detector distance of ~4.0 cm. The collected frames were integrated using an orientation matrix determined from the narrow frame scans. Apex II and SAINT software packages[37] were used for data collection and data integration. Analysis of the integrated data did not show any decay. Final cell constants were determined by global refinement of reflections from the complete data set. Data were corrected for systematic errors using SADABS[37] based on the Laue symmetry using equivalent reflections. Structure solutions and refinement were carried out using the SHELXTL-PLUS software package.[38] The structures were refined with full-matrix least-squares refinement by minimizing $\sum w(F_o^2 - F_c^2)^2$. All non-hydrogen atoms were refined anisotropically to convergence. All H atoms were added in the calculated position and were refined using appropriate riding models (AFIX m3). Selected crystals data and structure refinement parameters are listed in Tables 1 and 2. All data were collected at 100 K, except complex **7** for which data were collected at both 100 and 300 K. For the structural characterization of **7**, multiple data sets were collected on different crystals at room temperature and at 100 K. The perchlorate anion in the structure of **7** is disordered and sits on a 2-fold rotation axis. To be able to resolve the disorder, the symmetry equivalent atoms were generated and refined with half the expected occupancies and with PART-1/-2 instructions. The Ni(Me_4cyclam) fragment of the complex shows whole molecule disorder and the disorder was modeled as two overlapping motifs. The relative occupancies were refined using free variables. The disordered atoms were refined with geometrical restraints and displacement parameter restraints as listed in the .CIF file.

Synthesis of ligands

The *N*,*N*′-bis(salicylidene)-1,2-ethylenediimine (H_2salen1) and *N*,*N*′-bis(salicylidene)-1,2-propylenediimine (H_2salen2) ligands were synthesized by stirring 2 equiv. of 1,2-ethyldiamine or 1,2-diaminopropane, respectively, and 1 equiv. of salicylaldehyde in ethanol for 2 h.[23] The final solution was used for the synthesis of the corresponding metal complexes.

Synthesis of 1,4,8,11-tetrametyl-1,4,8,11-tetraazacyclotetradecane (Me_4cyclam). The Me_4cyclam ligand was synthesized following a literature procedure,[25] with some slight modifications. A solution containing 1.5 g of cyclam (7.5 mmol), 8.5 mL of 98% aqueous formic acid, 6.6 mL of formaldehyde (38% aqueous solution) and 5 mL of water was refluxed for 24 h. The reaction mixture was diluted with 15 mL of water, transferred to a 100 mL beaker, and cooled in an ice-bath. A concentrated solution of sodium hydroxide (15 g of NaOH dissolved in 50 mL of water) was slowly added with stirring until pH > 12. The temperature of the solution was kept below 25 °C. The solution was then extracted with 5 × 50 mL portions of

$CHCl_3$, the extracts were combined and dried over sodium sulphate, and then were concentrated to yield an oily residue. The residue crystallized at 4 °C overnight and the product was dried under vacuum for 2 h at 50 °C. Yield 80%. ^{1}H NMR (δ, $CDCl_3$, 300 MHz): 1.643 (q, ^3J(H–H) = 7 Hz, 4H, H_a), 2.198 (s, 12 H, 4Me), 2.427 (m, 16 H, $H_{b,c}$). ESI-MS: *m*/*z* 257.3, 257.3 expected for $[Me_4cyclamH]^+$.

Synthesis of 1,4,8,11-tetraazacyclotetradecane-1-acetic acid terahydrochloride (cyclamAc·4HCl). The cyclamAcH ligand was synthesized following a literature procedure,[26] with some slight modifications. To 1 g (5 mmol) of cyclam dissolved in 15 mL of EtOH and 3 mL of H_2O, 48 mg (2 mmol) of LiOH and 186 mg (1 mmol) of ICH_2COOH dissolved in 4 mL of H_2O were added at 5 °C. The mixture was refluxed for 4 h. The EtOH was then evaporated, and the alkaline aqueous solution was treated with $CHCl_3$ (4 × 10 mL) to remove non-reacted cyclam. The aqueous solution was dried at vacuum. Addition of 2 mL of HCl and 2 mL of EtOH lead to precipitation of the protonated tetrachloride product, which can be converted to the free-base form upon neutralization with NaOH. Yield: 41%. ^{1}H NMR (δ, $CDCl_3$, 300 MHz): 1.94 (m, 4H, H_a), 2.8–3.5 (m, 16 H, $H_{b,c}$), 3.6 (s, 2H, CH_2COOH). ESI-MS: *m*/*z*: 259.19, 259.21 expected for $[cyclamAcH]^+$.

Synthesis of metal–azide complexes

(a) Derived from salen ligands

Synthesis of [(salen1)Co^{III}(N$_3$)]$_2$. To a solution of H_2Salen1 (27 mg, 0.1 mmol) in EtOH heated at 60 °C, a solution of $Co(OAc)_2{\cdot}4H_2O$ (20 mg, 0.1 mmol) in 5 mL of EtOH and an aqueous solution (2 mL) of NaN_3 (6.5 mg, 0.1 mmol) were added. The solution was stirred at 60 °C for 30 min to form a brown precipitate. The reaction was cooled to room temperature and the solid was collected by filtration. X-Ray quality crystals were obtained by slow evaporation of the resulting solution in air. Yield: 91%. FTIR (NaCl, cm^{-1}): 2015(ν(N_3)), 1645, 1557 (ν(C═N)), 1471, 1447, 1338 (ν(C–N)), 1287. UV-Vis recorded in MeCN, λ_{max}/nm (ε/M^{-1} cm^{-1}): 390 (8300), 314 (12 400), 257 (43 000). Anal. Calc. for $C_{32}H_{28}Co_2N_{10}O_4{\cdot}7H_2O$ (MW 860.60): C, 44.66; H, 4.92; N, 16.28. Found: C, 44.57; H, 4.70; N, 16.00%. ESI-MS: *m*/*z* 325.00, 325.04 expected for $[(salen1)Co^{III}]^+$; 692.09, 692.10 expected for $[(salen1)Co^{III}N_3Co^{III}(salen1)]^+$.

Synthesis of [(salen2)Fe^{III}(N$_3$)]$_2$. To a solution of H_2Salen2 (57 mg, 0.2 mmol), an ethanol solution (10 mL) of $Fe(NO_3)_3{\cdot}9H_2O$ (80.8 mg, 0.2 mmol) and an aqueous solution (4 mL) of NaN_3 (13 mg, 0.2 mmol) were added under stirring. After allowing the resulting purple solution to stand in air for 10 days, black crystals were formed upon slow evaporation of the solvent. Yield: 77%. FTIR (NaCl, cm^{-1}): 2926, 2355 (ν(C–H)), 2058(ν(N_3)), 1618, 1598, 1541 (ν(C═N)), 1468, 1444, 1391 (ν(C–N)), 1299. UV-Vis recorded in MeCN, λ_{max}/nm (ε/M^{-1} cm^{-1}): 454 (2575), 319 (6167), 294 (sh) 256 (13 500). Anal. Calc. for $C_{34}H_{32}Fe_2N_{10}O_4{\cdot}4CH_3CH_2OH{\cdot}2H_2O$ (MW 976.68): C, 51.65; H, 6.19; N, 14.34. Found: C, 52.11; H, 5.85; N, 13.94%. ESI-MS: *m*/*z* 336.05, 336.08 expected for $[(salen2)Fe^{III}]^+$.

(b) Derived from cyclam ligands

Synthesis of [(Me$_4$cyclam)Ni^{II}(N$_3$)] (X = ClO$_4^-$ or PF$_6^-$): [(Me$_4$cyclam)Ni^{II}(N$_3$)]ClO$_4$[27a,b] To a stirred solution of Me_4cyclam (100 mg, 0.4 mmol) in 5 mL of ethanol was added an aqueous solution (5 mL) of NaN_3 (100 mg, 1.5 mmol). After 1 min, solid $Ni(ClO_4)_2{\cdot}6H_2O$ was added to the stirred solution (142.85 mg, 0.4 mmol). The solution was heated to 70 °C and stirred for 1 h. The resulting light green solution was cooled to room temperature, filtered to remove the excess NaN_3, and then kept at 4 °C. After 48 h, green needle crystals formed. Yield: 60%. FTIR (NaCl, cm^{-1}): 3392, 2996, 2939, 2864 (ν(C–H)), 2070 (ν(N_3)), 1471, 1433, 1324, 1307 (ν(C–N)), 1288, 1240, 1088 (ν(ClO_4^-)). UV-Vis recorded in MeCN, λ_{max}/nm (ε/M^{-1} cm^{-1}): 683 (85), 375 (2450). Anal. Calc. for $C_{14}H_{32}NiN_7ClO_4$ (MW 456.59): C, 36.83; H, 7.06; N, 21.47. Found: C, 36.79; H, 7.62; N, 21.46%. ESI-MS: *m*/*z* 359.16, 359.20 expected for $[(Me_4cyclam)Ni^{II}(N_3)]^+$.

Using the same procedure but starting with $Ni(NO_3)_2{\cdot}6H_2O$ and upon addition of an excess of KPF_6, the complex $[(Me_4cyclam)Ni^{II}(N_3)]PF_6$ was formed as green needle crystals suitable for X-ray crystallography. ESI-MS (*m*/*z*): 359.16, 359.20 expected for $[(Me_4cyclam)Ni^{II}(N_3)]^+$.

Synthesis of [(Me$_4$cyclam)Co^{II}(N$_3$)]]ClO$_4$[27c] To a stirred solution of Me_4cyclam (100 mg, 0.4 mmol) in 5 mL of ethanol was added an aqueous solution (5 mL) of NaN_3 (100 mg, 1.5 mmol). After 1 min, solid $Co(ClO_4)_2{\cdot}6H_2O$ was added to the stirred solution (143 mg, 0.4 mmol). The solution was heated at 70 °C and stirred for 1 h. The resulting dark-purple solution was cooled to room temperature, filtered to remove the excess NaN_3, and then kept at 4 °C. After 48 h, dark-purple crystals formed. Yield: 67%. FTIR (NaCl, cm^{-1}): 3014, 2925, 2867 (ν(C–H)), 2070 (ν(N_3)), 1476, 1089, 1275. UV-Vis recorded in MeCN, λ_{max}/nm (ε/M^{-1} cm^{-1}): 597 (118), 337 (2973). Anal. Calc. for $C_{14}H_{32}CoN_7ClO_4$ (MW 456.83): C, 36.81; H, 7.06; N, 21.46. Found: C, 36.35; H, 7.06; N, 21.45%. ESI-MS: *m*/*z* = 358.16, 358.21 expected for $[(Me_4cyclam)Co^{II}(N_3)]^+$.

Synthesis of [(cyclamAc)Fe^{III}(N$_3$)]PF$_6$[22] To 150 mg of cyclamAcH (0.58 mmol) dissolved in 5 mL degassed water was added 94.73 mg (0.58 mmol) of $FeCl_3$ in 5 mL degassed water. The resulting solution was brought to a gentle reflux and heated for 90 min as an orange color developed. The solution was cooled to room temperature and excess NaN_3 was added (124 mg, 1.9 mmol) to yield a dark-red solution. The resulting solution was stirred for 2 h at room temperature and subsequently filtered to yield a clear red filtrate. Addition of an aqueous solution (5 mL) of 350 mg KPF_6 (1.9 mmol) yielded red–orange microcrystals upon cooling at 4 °C overnight that were collected by filtration, washed with 2 × 10 mL diethyl ether, and dried under vacuum. Yield: 45%. FTIR (NaCl, cm^{-1}): 3260 (ν (N–H)), 2046 (ν(N_3)), 1651 (ν(C═O)), 838, 558 (ν(PF_6^-)). UV-Vis recorded in MeCN, λ_{max}/nm (ε/M^{-1} cm^{-1}): 460 (2500), 305 (4535), 276 (sh), 245 (11175). ESI-MS: *m*/*z* = 355.18, 355.14 expected for $[(cyclamAc)Fe^{III}(N_3)]^+$.

Synthesis of [(cyclamAc)Co^{III}(N$_3$)]ClO$_4$. To 150 mg of cyclamAcH (0.58 mmol), dissolved in 5 mL degassed water was added 214.41 mg (0.58 mmol) of $Co(ClO_4)_2{\cdot}6H_2O$ in 5 mL degassed water. The resulting solution was brought to a gentle reflux and heated for 90 min as an orange color developed. The solution was cooled to room temperature and an excess of NaN_3

was added (124 mg, 1.9 mmol) to yield a dark-purple solution. The resulting solution was concentrated to 2 mL and excess NaN_3 was filtered. The solvent was then removed and the purple product was washed with 2 × 10 mL diethyl ether, collected by filtration, and dried under vacuum. X-ray quality crystals were obtained by slow diffusion of ether into a MeCN solution. Yield: 50%. FTIR (NaCl, cm^{-1}): 2923 (ν(N–H)), 2052 ($\nu(N_3)$), 1686 (ν(C═O)), 837, 560. UV-Vis recorded in MeCN, λ_{max}/nm (ε/M^{-1} cm^{-1}): 545 (200), 317 (4727). Anal. Calc. for $C_{12}H_{25}ClCoN_7O_6{\cdot}7H_2O$ (MW 581.85): C, 24.77; H, 6.41; N, 16.85. Found: C, 24.44; H, 6.18; N, 16.76%. ESI-MS: m/z = 358.18, 358.14 expected for $[(cyclamAc)Co^{III}(N_3)]^+$.

Synthesis of metal–triazolate complexes

Synthesis of $\{(Me_4cyclam)Ni^{II}[N_3C_2(CO_2Me)_2]\}ClO_4$. To 10 mg $[(Me_4cyclam)Ni^{II}(N_3)]ClO_4$ (0.02 mmol) dissolved in chloroform were added 14 µl of dimethyl acetylenedicarboxylate (0.11 mmol). The solution was stirred for 6 h and the formation of the triazolate product was followed by FT-IR. The product was precipitated in hexane, filtered, and dried under vacuum. X-Ray quality crystals were obtained by slow diffusion of hexane into a dichloromethane solution at 4 °C. Yield: 91%. FTIR (NaCl, cm^{-1}): 2955, 2870, 1726 (ν(C═O)), 1480 (ν(N═N)), 1441, 1328, 1270 (ν(C–O), 1202, 1171, 1090, 964, 826, 806, 778, 750, 623. UV-Vis recorded in MeCN, λ_{max}/nm (ε/M^{-1} cm^{-1}): 636 (88), 514 (149), 386 (731). Anal. Calc. for $C_{20}H_{38}ClNiN_7O_8{\cdot}0.5C_6H_{14}$ (MW 641.79): C, 43.04; H, 7.07; N, 15.28. Found: C, 43.01; H, 6.93; N, 15.34%. ESI-MS: m/z = 498.30, 498.23 expected for $\{(Me_4cyclam)Ni^{II}[N_3C_2(CO_2Me)_2]\}^+$.

Synthesis of $\{(Me_4cyclam)Co^{II}[N_3C_2(CO_2Me)_2]\}ClO_4$. To 10 mg $[(Me_4cyclam)Co^{II}(N_3)]ClO_4$ (0.02 mmol) dissolved in chloroform were added 14 µl of dimethyl acetylenedicarboxylate (0.11 mmol). The solution was stirred for 10 h and the formation of the triazolate product was followed by FT-IR. The product complex was precipitated in hexane, filtered, and dried under vacuum. X-ray quality crystals were obtained by slow diffusion of hexane into a dichloromethane solution at room temperature. Yield: 84%. FTIR (NaCl, cm^{-1}): 2961, 2923, 2861, 2064, 1728 (ν(C═O)), 1479 (ν(N═N)), 1454, 1302, 1261, 1226 (ν(C–O), 1170, 1090, 1042, 1019, 960, 842, 822, 806, 779, 732, 623 cm^{-1}. UV-Vis recorded in MeCN, λ_{max}/nm (ε/M^{-1} cm^{-1}): 552 (30), 483 (43), 325 (sh). Anal. Calc. for $C_{20}H_{38}ClCoN_7O_8{\cdot}2H_2O$ (MW 616.97): C, 38.83; H, 6.67; N, 15.44. Found: C, 38.42; H, 6.39; N, 15.35%. ESI-MS: m/z = 499.16, 499.23 expected for $\{(Me_4cyclam)Co^{II}[N_3C_2(CO_2Me)_2]\}^+$.

Acknowledgements

We thank the Department of Chemistry at Washington University for start-up funds, the Department of Defense, Breast Cancer Research Program for a Concept Award (BC097014) to L. M. M., and the National Science Foundation (MRI, CHE-0420497) for the purchase of the ApexII diffractometer. E. E. thanks the Generalitat de Catalunya and Program Fulbright for a one-year Fulbright Fellowship Award. We also thank Barrie Cascella for the synthesis of propargyl amine substrates. L. M. M. is a Sloan Fellow.

Notes and references

1 H. C. Kolb, M. G. Finn and K. B. Sharpless, *Angew. Chem., Int. Ed.*, 2001, **40**, 2004.
2 (*a*) R. Huisgen, *Proc. Chem. Soc.*, 1961, 357; E. Lieber, R. L. Minnis and C. N. R. Lao, *Chem. Rev.*, 1965, **65**, 377; (*b*) R. Huisgen, G. Szeimies and L. Möbius, *Chem. Ber.*, 1976, **100**, 2949; (*c*) *The Chemistry of Azido Group*, ed. S. Patai, Interscience, New York, 1971.
3 (*a*) K. Nomiya, R. Noguchi and M. Oda, *Inorg. Chim. Acta*, 2000, **298**, 24; (*b*) S. S. van Berkel, A. J. Dirks, M. J. Debets, F. L. van Delft, J. J. L. M. Cornelissen and F. P. J. T. Tutjes, *ChemBioChem*, 2007, **8**, 1504; (*c*) A. Tam, U. Arnold, M. B. Soellner and R. T. Raines, *J. Am. Chem. Soc.*, 2007, **129**, 12670; (*d*) E. Bokor, T. Docsa, P. Gergely and L. Somsák, *Bioorg. Med. Chem.*, 2010, **18**, 1171; (*e*) E. M. Sletten and C. R. Bertozzi, *Acc. Chem. Res.*, 2011, **44**, 666.
4 (*a*) R. P. Singh, R. D. Verma, D. T. Meshri and J. M. Shreeve, *Angew. Chem., Int. Ed.*, 2006, **45**, 3584; (*b*) B. C. Tappan, M. H. Huynh, M. A. Hiskey, D. E. Chavez, E. P. Luther, J. T. Mang and S. F. Son, *J. Am. Chem. Soc.*, 2006, **128**, 6589.
5 (*a*) C. W. Tornoe, C. Christensen and M. Meldal, *J. Org. Chem.*, 2002, **67**, 3057; (*b*) V. V. Rostovtsev, L. G. Green, V. V. Fokin and K. B. Sharpless, *Angew. Chem., Int. Ed.*, 2002, **41**, 2596.
6 R. A. Copeland, M. R. Harpel and P. J. Tummino, *Expert Opin. Ther. Targets*, 2007, **11**, 967.
7 W. G. Lewis, L. G. Green, F. Grynszpan, Z. Radić, P. R. Carlier, P. Taylor, M. G. Finn and K. B. Sharpless, *Angew. Chem., Int. Ed.*, 2002, **41**, 1053.
8 (*a*) H. C. Kolb and K. B. Sharpless, *Drug Discovery Today*, 2003, **8**, 1128; (*b*) S. K. Mamidyala and M. G. Finn, *Chem. Soc. Rev.*, 2010, **39**, 1252; (*c*) X. Hu and R. Manetsch, *Chem. Soc. Rev.*, 2010, **39**, 1316.
9 T. Suzuki, Y. Ota, Y. Kasuya, M. Mutsuga, Y. Kawamura, H. Tsumoto, H. Nakagawa, M. G. Finn and N. Miyata, *Angew. Chem., Int. Ed.*, 2010, **49**, 6817.
10 There are several previous reports describing the cycloaddition reaction between metal–azide complexes and alkynes, and the term "inorganic click reaction" has been introduced before. Our current study reports cycloaddition reactions between first-row metal–azide complexes and an alkyne as a proof-of-concept for an enzyme-templated cycloaddition reaction as a novel strategy to synthesize metalloenzyme inhibitors. In this context, the proposed metalloenzyme-templated reaction is an inorganic variant of the *in situ* click reaction employed by Sharpless *et al*. in enzyme inhibitor design (ref. 7).
11 (*a*) T. Kemmerich, J. H. Nelson, N. E. Takach, H. Boehme, B. Jablonski and W. Beck, *Inorg. Chem.*, 1982, **21**, 1226; (*b*) B. T. Hsieh, J. H. Nelson, E. B. Milosavljevic, W. Beck and T. Kemmerich, *Inorg. Chim. Acta*, 1987, **133**, 267.
12 P. Paul and K. Nag, *Inorg. Chem.*, 1987, **26**, 2969.
13 M. Herberhold, A. Goller and W. Z. Milius, *Z. Anorg. Allg. Chem.*, 2003, **629**, 1162.
14 C. W. Chang and G. H. Lee, *Organometallics*, 2003, **22**, 3107.
15 L. Busetto, F. Marchetti, S. Zacchini and V. Zanotti, *Inorg. Chim. Acta*, 2005, **358**, 1204.
16 (*a*) K. S. Singh, C. Thone and M. R. Kollipara, *J. Organomet. Chem.*, 2005, **690**, 4222; (*b*) K. S. Singh, V. Svitlyk and Y. Mozharivskyj, *Dalton Trans.*, 2011, **40**, 1020.
17 J. A. K. Bauer, T. M. Becker and M. Orchin, *J. Chem. Crystallogr.*, 2004, **34**, 843.
18 (*a*) D. V. Partyka, J. B. Updegraff, M. Zeller, A. D. Hunter and T. G. Gray, *Organometallics*, 2007, **26**, 183; (*b*) D. V. Partyka, L. Gao, T. S. Teets, J. B. Updegraff, N. Deligonul and T. G. Gray, *Organometallics*, 2009, **28**, 6171.
19 K. Pachhunga, P. J. Carroll and K. M. Rao, *Inorg. Chim. Acta*, 2008, **361**, 2025.
20 F. C. Liu, Y. L. Lin, P. S. Yang, G. H. Lee and S. M. Peng, *Organometallics*, 2010, **29**, 4282.
21 T. J. Del Castillo, S. Sarkar, K. A. Abboud and A. S. Veige, *Dalton Trans.*, 2011, **40**, 8140.
22 C. G. Grapperhaus, B. Mienert, E. Bill, T. Weyhermüller and K. Wieghardt, *Inorg. Chem.*, 2000, **39**, 5306.

23 (*a*) Z.-D. Liu, M.-Y. Tan and H.-L. Zhu, *Acta Crystallogr., Sect. E: Struct. Rep. Online*, 2004, **60**, m910; (*b*) Z.-L. You and H.-L. Zhu, *Acta Crystallogr., Sect. E: Struct. Rep. Online*, 2004, **60**, m1046.
24 M. Weil and A. D. Khalaji, *Anal. Sci.*, 2008, **24**, x19.
25 E. K. Barefield and F. Wagner, *Inorg. Chem.*, 1973, **12**, 2435.
26 M. Struder and T. A. Kaden, *Helv. Chim. Acta*, 1986, **69**, 2081.
27 For the Ni complex: (*a*) A. Escuer, R. Vicente, M. S. El Fallah, X. Solans and M. Font-Bardia, *Inorg. Chim. Acta*, 1996, **247**, 85; (*b*) M. J. D'Aniello Junior, M. T. Mocella, F. Wagner, E. K. Barefield and I. C. Paul, *J. Am. Chem. Soc.*, 1975, **97**, 192. For the Co complex: (*c*) S. Reiner, M. Wicholas, B. Scott and R. D. Willett, *Acta Crystallogr., Sect. C: Cryst. Struct. Commun.*, 1989, **45**, 1694.
28 B. Bosnich, C.-K. Poon and M. L. Tobe, *Inorg. Chem.*, 1965, **4**, 1102.
29 (*a*) A. W. Addison, T. N. Rao, J. Reedijk, J. Van Rijn and G. C. Verschoor, *J. Chem. Soc., Dalton Trans.*, 1984, 1294; (*b*) R. D. Willett, G. Pon and C. Nagy, *Inorg. Chem.*, 2001, **40**, 4342.
30 P. V. Bernhardt and G. A. Lawrance, *Coord. Chem. Rev.*, 1990, **104**, 297–343.
31 M. Costas, M. P. Mehn, M. P. Jensen and L. Que Jr., *Chem. Rev.*, 2004, **104**, 939.
32 The Cambridge Structural Database, http://www.ccdc.cam.ac.uk/, search performed December 2011.
33 J. H. Nelson, N. E. Takach, N. Bresciani-Pahor, L. Randaccio and E. Zangrando, *Acta Crystallogr., Sect. C: Cryst. Struct. Commun.*, 1984, **40**, 742.
34 A. Clearfield, R. Gopal, R. J. Kline, M. L. Sipski and L. O. Urban, *J. Coord. Chem.*, 1978, **8**, 5.
35 (*a*) Y. Zhang and R. J. Klose, *Nat. Rev. Mol. Cell Biol.*, 2007, **8**, 307; (*b*) A. Spannhoff, A.-T. Hauser, R. Heinke, W. Sippl and M. Jung, *ChemMedChem*, 2009, **4**, 1568; (*c*) N. R. Rose, M. A. McDonough, O. N. F. King, A. Kawamura and C. J. Schofield, *Chem. Soc. Rev.*, 2011, **40**, 4364.
36 (*a*) L. A. Boyer, K. Plath, J. Zeitlinger, T. Brambrink, L. A. Medeiros, T. L. Lee, S. S. Levine, M. Wernig, A. Tajonar, M. K. Ray, G. W. Bell, A. P. Otte, M. Vidal, D. K. Gifford, R. A. Young and R. Jaenisch, *Nature*, 2006, **441**, 349; (*b*) P. A. C. Cloos, J. Christensen, K. Agger, A. Maiolica, J. Rappsilber, T. Antal, K. H. Hansen and K. Helin, *Nature*, 2006, **442**, 307.
37 Bruker Analytical X-Ray, Madison, WI, 2008.
38 G. M. Sheldrick, *Acta Crystallogr., Sect. A: Found. Crystallogr.*, 2007, **64**, 112.